IMPROVEMENT AND PRACTICAL APPLICATION OF SINGLE FIBER FRAGMENTATION TEST

by

Banu Taşlıca

B.S. in Chemistry, Boğaziçi University, 2004

Submitted to the Institute for Graduate Studies in
Science and Engineering in partial fulfillment of
the requirements for the degree of
Master Science
in
Chemistry

Graduate Program in Chemistry
Boğaziçi University
2007

IMPROVEMENT AND PRACTICAL APPLICATION
OF SINGLE FIBER FRAGMENTATION TEST

APPROVED BY:

Prof. Selim Küsefoğlu ……
(Thesis Supervisor)

Asist. Prof. Ersin Acar ……

Prof. Sabri Altıntaş ……

DATE OF APPROVAL: …….

To my family

and

To my dearest

ACKNOWLEDGEMENTS

First of all I am indebted to my thesis supervisor Prof. Dr. Selim Küsefoğlu for his guidance, suggestions and for all the support he has given me throughout my research and school life. It was great pleasure for me to work with him. I will carry the signs of his guidance all my life.

I would like to express my sincere gratitude to the members of committee; Dr. Ersin Acar and Prof. Sabri Altıntaş for reviewing the final manuscript and making helpful comments.

I would also like to thank all members of Chemistry Department for their encouragements and moral support during my study, especially Hülya Metiner, and my best friends Pınar Çakır, Nazende Günday, Damla Köylü and Kamer Sözer. My special thanks are for my laboratory partners Gökhan Çaylı and Cem Öztürk for their help and friendship. I also thank to Sinan Şen and Ayla Türkekul for their help in obtaining AFM images and NMR spectra.

My greatest thanks go to my family and to my boyfriend for their most valuable understanding, patience and moral support that they have given me during this study. Thank you very much.

ABSTRACT

IMPROVEMENT AND PRACTICAL APPLICATION OF SINGLE FIBER FRAGMENTATION TEST

The single fiber fragmentation test (SFFT) has been used to investigate the interphase in fiber-reinforced composites. However SFFT is still far from a routine test for industrial applications. The aim of this work is to turn SFFT into a practical, quick test. A new approach was developed for SFFT based on the usage of the maximum number of fragments on the fiber to compare different fiber-matrix interphase qualities. This approach does not involve length measurements and shortens the experiment time to few minutes. Test samples were prepared by using E-glass fibers with different commercial sizings and unsaturated polyester resin. SFFT results were in good agreement with the macromechanical test results. The crack modes and debonding phenomena were examined from the microscopic images. Atomic force microscope (AFM) images were examined to get a better knowledge about different fiber surfaces. New improvements were developed to get better interphase adhesive strength. The first improvement was done by adding methacryl silane as coupling agent to the matrix resin directly in different percentages. Higher percentages resulted with higher quality on the adhesive strength but decreased the mechanical properties of the matrix. The second improvement was done by addition of 3-aminopropyltriethoxysilane to unsaturated polyester via Michael addition reaction. Characterization of the product was done by ^{1}H NMR spectroscopy. The results of SFFT showed that the maximum numbers of fragments for the samples prepared from 3-aminopropyltriethoxysilylated polyester are quite high. That means better interphase quality was achieved by aminosilylated polyester matrix.

ÖZET

Tek lif parçalanma testi, elyaf takviyeli plastik kompozitlerin arayüzeylerini incelemek amacıyla kullanılmaktadır. Fakat test henüz yeni gelişmeleri incelemek amacıyla endüstriyel uygulamalarda kullanılabilen rutin bir test olmaktan uzaktır. Bu çalışmanın amacı tek lif parçalanma testini pratik ve çabuk bir test haline getirmektir. Bu çalışmada değişik ara yüzey kalitelerini karşılaştırmak amacıyla elyaftaki maksimum parça sayılarının kullanılmasına dayalı yeni bir yöntem geliştirilmiştir. Bu yöntem zahmetli uzunluk ölçümlerine gerek kalınmadan deneyi birkaç dakikaya indirmektedir. Bu çalışmadaki değişik ticari bağlaycıları (sizing) olan E-cam elyafları ile doymamış poliester reçinesi kullanılarak test örnekleri hazırlanmıştır. Tek lif parçalanma testi makromekanik test sonuçları ile uygun sonuçlar vermiştir. Mikroskop görüntüleri yardımıyla kırık çeşitleri ve ayrılma konusu üzerinde çalışılmıştır. Atomik kuvvet mikroskobu sonuçları kullanılarak elyaf yüzeyi hakkında daha fazla bilgi edinilmiştir. Atomik kuvvet mikroskobu sonuçlarına dayanarak daha iyi arayüzey bağlanma kuvveti elde etmek amacıyla yeni geliştirmeler yapılmıştır. İlk geliştirme matrikse bağlayıcı olarak değişik yüzdelerde metakrilsilan karıştırılması ile yapılmıştır. Yüksek yüzdeli örnekler bağlanma kuvvetini artırırken matriksin mekanik mukavemetini düşürmüştür. İkinci geliştirme 3-aminopropiltrietoksisilanın doymamış polyestere Michael katılma reaksiyonu ile bağlanmasıyla yapılmıştır. Ürünün karakterizasyonu ^{1}H NMR spektroskopi ile yapılmıştır. Tek lif parçalanma testi sonucunda, 3-aminopropiltrietoksisilan katılmış polyester ile yapılan test örneklerinde maksimum kırık sayıları oldukça yüksek çıkmıştır. Bu sonuç aminosilan katılmış polyester matriks ile daha kaliteli ara yüzey elde edildiğini göstermiştir.

TABLE OF CONTENTS

ACKNOWLEDGEMENTS iv
ABSTRACT v
ÖZET vi
LIST OF FIGURES ix
LIST OF TABLES xii
LIST OF SYMBOLS / ABBREVIATIONS xiii
1. INTRODUCTION 1
1.1. Fiber Reinforced Polymer Composites 1
1.2. Properties of FRP Composites 3
1.3. Constituents of Composites 6
1.3.1. Reinforcements 6
1.3.2. Matrix materials 9
1.4. Interphase Between Glass Fibers and the Matrix 11
1.4.1 Sizing 13
1.4.2. Organofunctional Silanes 14
1.5. Evaluation of Interfacial Adhesive Strength 19
1.6. Micromechanical Test with Single Fiber 20
1.6.1. Microbond Test 21
1.6.2. Microindentation Test 22
1.7. Background of Single Fiber Fragmentation Test (SFFT) 23
1.8. Multiple Fiber Fragmentation Test 28
1.9. Observations on Fiber Fracture Modes and Interfacial Debonding Phenomena. 28
1.10. Atomic Force Microscopic Images of Fiber Surfaces 31
1.11. Attempts to Improve Interfacial Adhesive Strength Between Glass Fiber and Unsaturated Polyester 32
2. STATEMENT OF THE PROBLEM 35
3. RESULTS AND DISCUSSIONS 36
3.1. Behavior of the fibers during SFFT 36
3.2. Comparing SFFT results with the Macromechanical test results 37
3.3. Results for other commercial fibers 41

3.4. Results for Unsized and Improperly Sized Fibers 43
3.5. Observation of different modes of fractures and debonding phenomena 44
3.6. Multiple fiber fragmentation test results 46
3.7. AFM results 48
3.8. Methacryl silane addition into matrix mixture 50
3.9. Michael addition of aminosilane to unsaturated polyester 52
4. EXPERIMENTAL 57
4.1. Chemicals and Apparatus 57
4.1.1. Chemicals 57
4.1.2. Apparatus 59
4.1.2.1. Apparatus for Sample Preparation. 59
4.1.2.2. Apparatus for Testing. 60
4.1.3. Characterization Instruments 62
4.2. Sample Preparation and Testing 62
4.2.1. Sample Fabrication 62
4.2.1.1. Fiber Lay-up. 62
4.2.1.2. Matrix Casting and Curing. 63
4.2.2. Testing and Data Collection 64
4.2.3. Test samples with multiple glass fiber 65
4.2.4. Test samples with methacryl silane added matrix 65
4.2.5. Aminosilylation of unsaturated polyester 66
5. CONCLUSIONS 67
REFERENCES 69

LIST OF FIGURES

Figure 1.1. Representation of tensile stress-strain curve for fiber, resin and FRP composites 3

Figure 1.2. Representation for the anisotropic behavior of fibers 4

Figure 1.3. A glass fiber strand 7

Figure 1.4. Two dimensional illustration of the polyhedron network structure of sodium silicate glass 7

Figure 1.5. Glass fiber surface structure 8

Figure 1.6. Schematic representation of the synthesis of unsaturated polyester 10

Figure 1.7. Acceleration of the formation of free radicals by cobalt metal [7]. 11

Figure 1.8. Illustration for fiber-matrix and their interphase 12

Figure 1.9. Schematic diagram of fiber manufacturing 13

Figure 1.10. General formula of organofunctional silanes 14

Figure 1.11. Representation of binding process of polymer to glass fiber surface by the help of silane 15

Figure 1.12. Functions of organofunctional silane as a coupling agent 16

Figure 1.13. Structure of methacryl silane 16

Figure 1.14. Mechanism of the reaction of methacryl silane with unsaturated polyester and styrene 17

Figure 1.15. Structure of 3-Aminopropyltriethoxysilane 18

Figure 1.16. Mechanism of Michael addition of amino silane to unsaturated polyester . 19

Figure 1.17. A microbond test method 22

Figure 1.18. A microindentation test method 23

Figure 1.19. Dumbell shaped test specimen 24

Figure 1.20. (a) Dog-bone shape fiber fragmentation test specimen; (b) fiber 25

Figure 1.21. The fiber at the beginning and at the end of SFFT 26

Figure 1.22. Illustration of fragmentation process 26

Figure 1.23. Illustration of number of fractures versus elongation graph 27

Figure 1.24. Schematic representations of fiber crack and break gap..... 28

Figure 1.25. The three modes of fracture that arise in a single-fiber composite during a fragmentation experiment..... 29

Figure 1.26. Schematic debonding microstructure of fiber and matrix interphase. (a) Before loading (no fiber break); (b) After loading (fiber break). 30

Figure 1.27. Schematic feature of debond zone of E-glass fiber. (a) Loading-applied state; (b) Loading-released state. 31

Figure 1.28. Interphase of test sample with methacryl silane added matrix..... 33

Figure 1.29. Interphase of test sample with Michael adduct of aminosilane and polyester matrix 33

Figure 3.1. Number of fragments as a function of extension for the specimens with WR-5 and WR-4 36

Figure 3.2. SFFT results: Maximum numbers of fragments for WR-5, WR-4, and WR-3 38

Figure 3.3. Macromechanical test results: Normalized ultimate tensile strength of WR-5, WR-4, and WR-3 per glass per cent. 38

Figure 3.4. SFFT results: Maximum number of fragments for PPG, VT, and WR-5.... 42

Figure 3.5. Macromechanical test results: Normalized ultimate tensile strength for 1200 tex WR-5, PPG and VT 42

Figure 3.6. SFFT results: Maximum number of fragments for unsized GF, PP and WR-5 44

Figure 3.7. Fragmentation process of the specimen with WR-5, (a) at the beginning of the process, (b) in the middle of the process, (c) at the end of the process.. 45

Figure 3.8. Different fragment modes of WR-5..... 45

Figure 3.9. Fragmentation process for PP 46

Figure 3.10. Comparison of single fiber and multifiber fragmentation test results. 47

Figure 3.11. Multifiber test samples: (a) WR-5, (b) WR-3 47

Figure 3.12. Illustration for the scanning process of AFM..... 48

Figure 3.13. AFM image of (a) unsized and (b) sized glass fiber..... 49

Figure 3.14. SFFT results for WR-5, WR-5 with 3 per cent methacryl silane added polyester, and WR-5 with 5 per cent methacryl silane added polyester 51

Figure 3.15. Picture of WR-5 with aminosilylated CE-92 after the load applied..... 55

Figure 3.16. SFFT results for Unsized GF and WR-5 with CE-92 and aminosilylated CE-92 56

Figure 4.1. The silicone mold with eight dumbell shaped cavity 59

Figure 4.2. Dimensions of dumbell shaped specimen..... 60

Figure 4.3. Schematic illustration for testing system 60

Figure 4.4. Micro-straining device..... 61

Figure 4.5. Dimensions of micro-straining device..... 61

LIST OF TABLES

Table 1.1. Mechanical properties of traditional and advanced materials 2

Table 1.2. Mechanical properties of different fibers 8

Table 3.1. Macromechanical test for the samples with WR-5, WR-4 and WR-3..... 39

Table 3.2. Comparison of macromechanical test and SFFT results for the samples with WR-5, WR-4 and WR-3 40

Table 3.3. Per cent improvement achieved by methacryl silane addition 52

Table 3.4. Per cent improvement achieved aminosilylated CE-92 56

Table 4.1. Chemicals and suppliers..... 57

Table 4.2. Properties of UPE CE 92..... 58

Table 4.3. Properties of E-glass fiber 58

LIST OF SYMBOLS / ABBREVIATIONS

μ	Coefficient of friction / distance
ρ	Density
σ	Tensile strength
σ^z_f	Axial stress profile
τ_b	Shear strength
τ_{fr}	Frictional strength
E	Tensile modulus
E_f	Young's modulus
G_{ic}	Fracture toughness
P	Applied force
q_0	Clamping stress
A1100	Commercial name of 3-aminopropyltriethoxysilane
AFM	Atomic force microscopy
ASTM	American Society for Testing and Materials
C-glass	Chemical/corrosion grade glass
CE 92 N8	Commercial name of a UPE resin dissolved in styrene
Co-Naphtenate	Cobalt-Naphtenate (catalyst)
E-glass	Electrical grade glass
FRP	Fiber-reinforced polymer
MEKP	Methyl ethyl ketone peroxide (accelerator)
SFFT	Single fiber fragmentation test
S-glass	Structural grade glass
PPG	Pittssburg Plate Glass
RT	Room temperature
UPE	Unsaturated polyester
VT	Vetrotex
WR-3/4/5	Commercial name of the glass fibers

1. INTRODUCTION

1.1. Fiber Reinforced Polymer Composites

Engineers have many choices of materials to design and manufacture products for various applications. A lot of research has been done to develop composites with higher strength and higher fracture toughness, lighter weight and lower cost compared to the more traditional structural materials such as metals. Fiber-reinforced plastics (FRP) are composite materials that have been developed to solve technological problems of traditional materials. They consist of high strength and high modulus fiber and a low modulus polymeric matrix. The strength of the final composite depends largely on the strength of the fiber and the interfacial adhesion between the fiber and the matrix.

Table 1.1 shows the mechanical properties of traditional and advanced materials. From the values in the Table it is observed that plastics have mechanical properties that are between metals and ceramics. But when they are reinforced with fibers either with short fibers or with unidirectional continuous fibers, the mechanical properties become much better.

Characterization of these new composite materials is required by testing their mechanical properties. In the industrial environment these tests include preparation of many samples and testing their tensile, flexural and impact properties on universal testing machines. These tests are called as macromechanical tests. Unfortunately, it is difficult to get unambiguous results when testing bulk composites with macromechanical tests because the errors in the microscopic level can not be eliminated. These errors are the voids in the sample and differences in cure rates within the sample. Consequently, several micromechanical techniques have been developed, which try to measure the interfacial shear strength correctly based on first principles. One of these micromechanical tests is

single fiber fragmentation test (SFFT) [1]. This work is an effort to turn the SFFT to a practical and fast test to be used in industrial applications.

Table 1.1. Mechanical properties of traditional and advanced materials [2]

Material	Density (ρ) (G/cc)	Tensile modulus (E) (GPa)	Tensile strength (σ) (GPa)	Specific modulus (E/ρ)	Specific Strength (σ/ρ)	Maximum Service Temp. (°C)
Metals						
Cast iron	7.0	100	0.14	14.3	0.02	230-300
Steel	7.8	205	0.57	26.3	0.073	500-650
Aluminum	2.7	73	0.45	27.0	0.17	150-250
Plastics						
Nylon 6/6	1.15	2.9	0.082	2.52	0.071	75-100
Polypropylene	0.9	14	0.033	1.55	0.037	50-80
Epoxy	1.25	3.5	0.069	2.8	0.055	80-215
Ceramics						
Alumina	3.8	350	0.17	92.1	0.045	1425-1540
MgO	3.6	205	0.06	56.9	0.017	900-1000
Short Fiber composites						
Glass-filled epoxy (35%)	1.90	25	0.30	8.26	0.16	80-200
Glass-filled polyester (35%)	2.00	15.7	0.13	7.25	0.065	80-125
Glass-filled nylon (35%)	1.62	14.5	0.20	8.95	0.12	75-110
Unidirectional composites						
S-glass/epoxy (45%)	1.81	39.5	0.87	21.8	0.48	80-215
Carbon/epoxy (61%)	1.59	142	1.73	89.3	1.08	80-215
Kevlar/epoxy (53%)	1.35	63.6	1.1	47.1	0.81	80-215

1.2. Properties of FRP Composites

Fiber-reinforced plastic (FRP) composites have been widely used as structural materials in automotive, boat, aircraft and aerospace industries where high specific strength is needed. Also they are used in appliances, consumer products, electronic components and infrastructure. The reason for this superior performance is the synergistic combination of more than one constituent phase. FRP composites are made of a polymer with lower strength reinforced with fibers of higher strength. In this form fibers and polymer retain their physical and chemical identities, and produce a combination of properties that can not be achieved with either of the constituents acting alone. In order to achieve a true reinforcement, the fiber, the load bearing component, has to have a high degree of interfacial adhesion to the matrix. This ensures stress transfer from the matrix to the fiber.

In many applications where performance is the controlling factor (e.g., aerospace, transportation, underwater vessels), advanced structural materials that are stronger, stiffer, lighter in weight, and more resistant to hostile environments are needed. Unreinforced materials available today cannot meet any of these requirements [3].

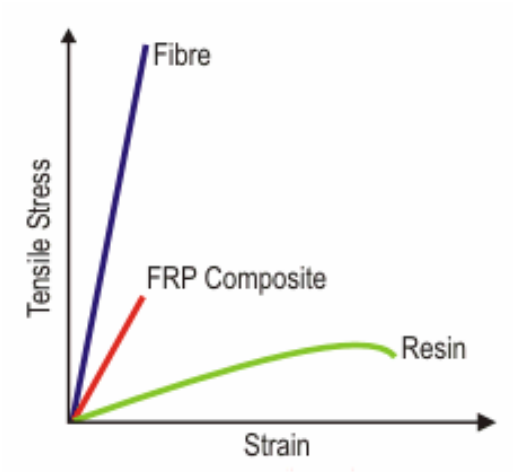

Figure 1.1. Representation of tensile stress-strain curve for fiber, resin and FRP composites

Figure 1.1 shows the stress-strain curve of a fiber, a typical resin and FRP composite. FRP composites have mechanical properties between fiber and polymers.

It is worth remembering that composites are less likely than metals (such as aluminum) to break up catastrophically under stress. A small crack in a piece of metal can propagate very rapidly leading to very serious consequences (especially in the case of aircraft). The fibers in the composite act to block the propagation of small cracks and distribute the stress over a wider region. Therefore FRPs have very high fracture toughness.

The design of a fiber-reinforced structure is different than that of a metal structure, because of the difference in its properties in different directions. Fibers show anisotropic behavior which means that the mechanical property depends on the direction. This behavior is represented in Figure 1.2. Both the tensile strength and the tensile modulus are higher in the direction of the fibers. Also the anisotropic nature of a FRP composite material creates a unique opportunity for tailoring its properties according to the design requirements. This design flexibility of FRP composites can be used to selectively reinforce a structure in the directions of major stresses, increase its stiffness in a preferred direction. This is a strategy that nature uses in wood which is four times stronger in the fiber direction than in the perpendicular direction.

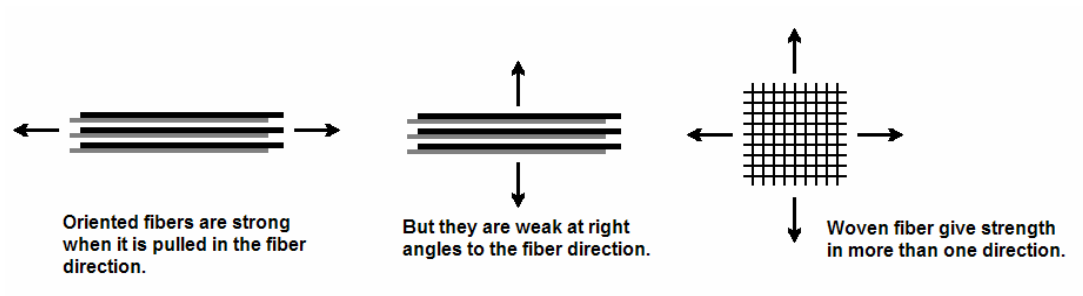

Figure 1.2. Representation for the anisotropic behavior of fibers

In addition to directional dependence of properties, there are number of other differences between structural metals and FRP composites. For example metals in general exhibit yielding and plastic deformation. Most FRP composites are elastic in their tensile stress-strain characteristics. However, the heterogeneous nature of these materials provides mechanisms for high-energy absorption on microscopic scale comparable to the yielding process. Mechanisms of damage development and growth in metal and composite structures are also quite different [3].

Another unique characteristic of many FRP composites is their high degree of internal damping. They have better vibrational energy absorption within the material and reduced transmission of noise and vibrations to neighboring structures. The high damping of composite materials can be beneficial in many automotive applications in which noise and vibration are critical issues for passenger comfort [3].

The other advantage of FRP composites is their resistance to corrosion. A typical polyester-glass fiber boat hull retains its useful strength in a salt water and high UV environment for 25 years. However many polymeric matrix composites are capable of absorbing moisture from the surrounding environment, which creates dimensional changes as well as adverse internal stresses within the material. If such behavior is undesirable in the application, the composite surface must be protected from moisture diffusion by appropriate paints or coatings [3].

The majority of past efforts have concentrated on the chemical aspect of fiber-matrix adhesion through the use of surface treatments and coatings. Most commercial fibers now available in the market are already treated and coated to improve the fiber matrix interfacial strength and to protect the fibers from environmental attacks such as moisture and reactive fluids.

The characteristics of the fiber-matrix interface play a critical role in the mechanical behavior of composite materials. In order to observe the difference in the interfacial strength of the fiber and matrix for different FRP composites, there have been recent reports describing experimental techniques and numerical models to determine the interfacial properties of composites. Among these techniques the most widely used

methods are the micro bond test, the micro indentation test and the single fiber fragmentation test.

Before examining these methods we should review the constituents and the structure of the interphase between the fiber and the matrix in FRP composites.

1.3. Constituents of Composites

The major constituents of a FRP composite material are the reinforcing fibers and the polymeric matrix that acts as a binder for the fibers. The interface of these materials is made of a special mixture of chemicals called sizing.

1.3.1. Reinforcements

Glass, carbon, aramid and boron fibers are the most common fibers used. All these fibers can be incorporated into a matrix either in continuous or in discontinuous (chopped) lengths. Fibers are thin rod like structures and their diameters range from 10 to 20 μm. Because of this thin diameter, the fiber is flexible and easily conforms to various shapes. But fibers are used as strands. Thanks to their flexibility, strands can be woven into textiles. Figure 1.3 shows a glass fiber strand.

Fibers have many functions in the composites. The most important one is to carry the load. In a structural composite, 70 to 90 per cent of the load is carried by fibers. The fiber has a tensile strength that is about 10 times greater than that of the matrix. And other functions of fibers are to provide stiffness, fracture toughness, thermal stability, and impact strength to the composites.

Figure 1.3. A glass fiber strand

Glass is found in abundance and glass fibers are the cheapest among all other types of fibers. A variety of chemical compositions of mineral glasses have been used to produce fibers. The most commonly used are silica (SiO_2) with additions of oxides of calcium, aluminum, iron, sodium and magnesium.

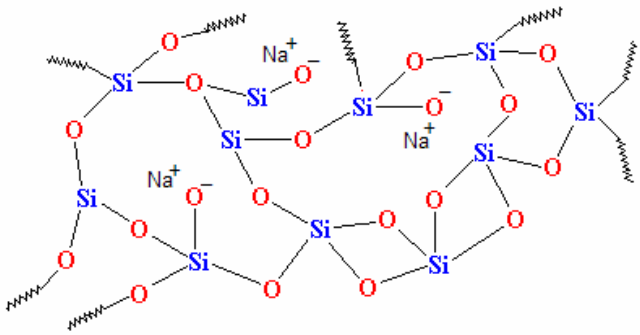

Figure 1.4. Two dimensional illustration of the polyhedron network structure of sodium silicate glass

The polyhedron network of sodium silicate glass is schematically illustrated in Figure 1.4, where each polyhedron is a combination of oxygen atoms around a silicon atom bonded by covalent bonds [1]. The sodium ions are not linked to the network, but only form ionic bonds with oxygen atoms.

Typical combinations of three most popular glass fibers are E, C and S-glass. The designations E, C and S stand for electrical, chemical/corrosion and structural grades, respectively. The different properties come from the amount of the metal oxides, for example E-glass is resistant to leaching in water and S-glass has highest strength and stiffness [4].

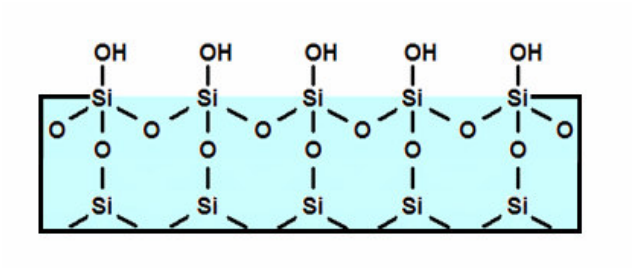

Figure 1.5. Glass fiber surface structure

The fiber used in this work is a glass fiber made of E-glass produced by Cam Elyaf A.Ş. in Çayırova, Gebze. Glass is an inorganic, polar and hydrophilic material that is made of silyl ethers in the bulk, but contains silanol groups at its surface which is illustrated in Figure 1.5.

Table 1.2. Mechanical properties of different fibers [2]

Fibers	Tensile modulus (E) (GPa)	Tensile strength (σ) (GPa)	Specific modulus (E/ρ)	Specific Strength (σ/ρ)	Melting Point (°C)	% Elongation at Break	Relative Cost
E-glass	70	3.45	27	1.35	1540+	4.8	Low
S-glass	86	4.50	34.5	1.8	1540+	5.7	Moderate
Graphite	240	2.6	140	1.5	>3500	0.8	High
Boron	400	3.5	155	1.3	2300	-	High
Kevlar	80	2.8	55.5	1.9	500(D)	3.5	Moderate

Table 1.2 shows the mechanical properties of different reinforcements. Although tensile modulus and specific modulus values for glass fibers are lower than other reinforcements, tensile strength and specific strength values for glass fibers are very high. Also they have good elongation at break values and lowest cost among the commercially available fibers.

1.3.2. Matrix materials

The matrix must keep the fibers in a desired location and orientation, separating fibers from each other to avoid mutual abrasion during periodic straining of the composite. The matrix acts as a load transfer medium between fibers, and in less ideal cases where loads are complex, the matrix may even have to bear loads transverse to the fiber axis. Since the matrix is generally more ductile than the fibers, it is the source of composite toughness. The matrix also serves to protect the fibers from environmental damage before, during, and after composite processing [5].

Composites are usually made from matrices of epoxy, unsaturated polyester, vinyl ester and a few thermoplastics. The matrix polymer used in this work is unsaturated polyester. Polyesters are thermosetting, low-cost resin systems and offer excellent corrosion protection and strength.

Unsaturated polyester resins used in reinforced plastics are a mixture of reactive polymers and reactive monomers. Unsaturated polyester resins are step growth polymers formed by the condensation polymerization of stoichiometric mixtures of unsaturated and saturated acids or anhydrides with dihydric alcohols. Acids can be maleic, fumaric, phthalic or terephthalic and the alcohols can be ethylene glycol, propylene glycol or halogenated glycol.

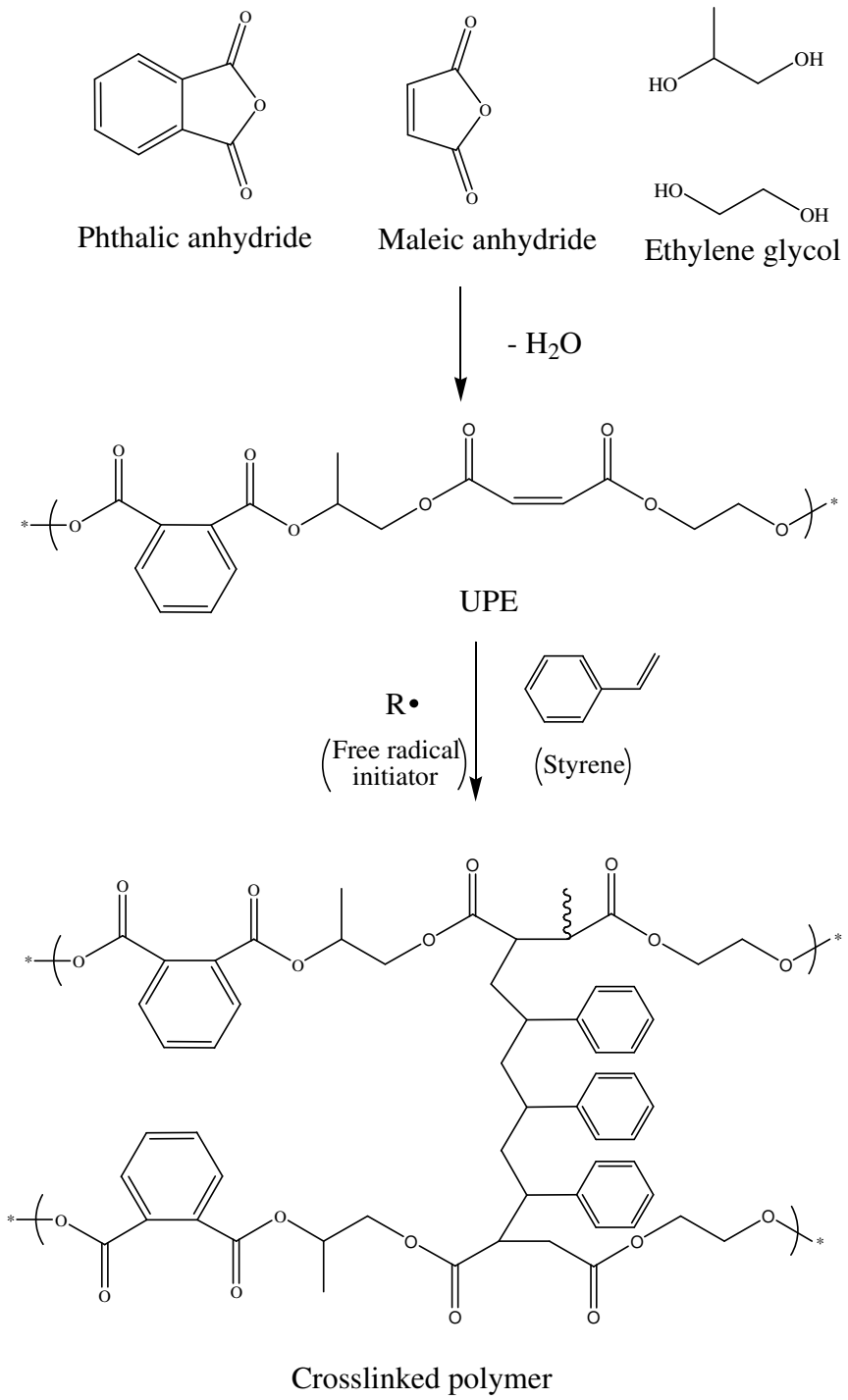

Figure 1.6. Schematic representation of the synthesis of unsaturated polyester

A typical synthesis is shown in Figure 1.6. Maleic anhydride is used to provide reactive double bonds used for crosslinking reaction. The resulting unsaturated polyester is dissolved in a reactive diluent such as styrene. A mixture of the styrene and unsaturated polyester and a free radical initiator is poured over a mass of glass fibers in a mold. The styrene and the double bonds in the polyester react by free radical polymerization to form a crosslinked resin. The glass fibers are embedded inside, where they act as a reinforcement.

The crosslinking reaction is carried out by adding free-radical catalysts to start the chain reaction of unsaturated polyester with styrene. Styrene combines with the reactive double bonds of the polyester chains, linking them together to form a strong three dimensional polymer network. The free radicals are derived from peroxides such as benzoyl peroxide and methyl ethyl ketone peroxide (MEKP) or from other unsTable materials, such as azo compounds, that can break into radical fragments. Most peroxide catalysts decompose rather slowly when added to the polyester resin. In order to get faster cure, accelerators (promoters), such as Cobalt-naphthenate, are used to speed up catalyst decomposition [6]. Dissociation of peroxide catalyst into free radicals involves a redox reaction with the accelerator as shown in Figure 1.7. This cycle is repeated until all the hydroperoxide has been decomposed.

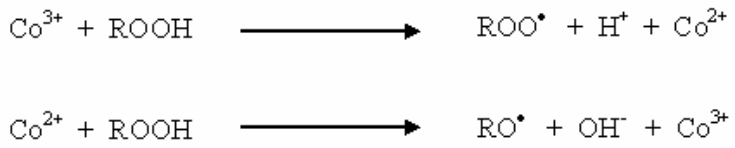

Figure 1.7. Acceleration of the formation of free radicals by cobalt metal [7].

1.4. Interphase Between Glass Fibers and the Matrix

Although bonding of organic polymers to inorganic surfaces has long been familiar operation (eg., protective coating on metals), a major need for new bonding techniques arose in 1940 when glass fibers were first used as a reinforcement in organic resins.

As pointed out by Bascom and Drzal [8], the term “adhesion” or “adhesion strength” is commonly used to describe the load or stress required to separate two dissimilar solids at or near their common boundary.

With the advent of magneticly triggered mines used by the Axis in the Second World War, the need for minesweepers made from non-ferrous materials arose. Electric Boat company, situated in Wisconsin, USA, made the first boat hulls from glass fiber reinforced polyester. The glass fiber had a coating of polyvinyl acetate to increase interfacial adhesion. These boats became an instant success in removing the magneticly triggered mines from the Atlantic Ocean.

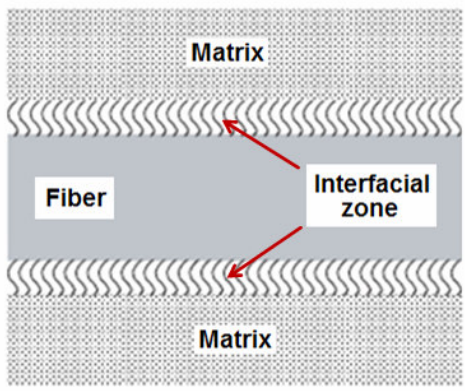

Figure 1.8. Illustration for fiber-matrix and their interphase

Figure 1.8 is an illustration for matrix, fiber and their interfacial zone where the adhesion takes place. Fiber-matrix adhesion can occur through five basic mechanisms: adsorption and wetting; mechanical interlocking; interdiffusion; dipolar and/or ionic inrteractions; and covalent bonding. It is believed that chemical bonding will lead to the strongest and environmentally sTable interfaces [9].

The problem is a classical problem of incompatibility between the organic, nonpolar polymer matrices and the inorganic, polar glass fiber.

1.4.1 Sizing

For glass fiber polymer composites, the interphase properties are improved by a surface coating, called sizing, which is applied to the glass fibers during manufacturing via an aqueous emulsion to ensure uniform coverage of the surface. The continuous glass fibers are generated from molten glass by being drawn through small orifices, as schematically shown in Figure 1.9. Sizing is used to protect the fibers from damage and provide compatibility with the matrix by providing a chemical link between fiber and matrix. The size is generally 0.1 to 1 μm thick, and must have adequate mechanical film properties, such as rigidity, tensile strength, and toughness, to carry the mechanical load when the composite is stressed. A typical glass fiber size mainly includes film-forming resin, antistatic agent, lubricant and coupling agent. It is necessary to apply "coupling agent", because it facilitates adhesion of polymers to fibers.

Covalent bonding, wetting, hydrogen bonding and Van der Waals force are the interactions in interphase of fiber-matrix composites by the help of coupling agents. Organofunctional silanes are used as coupling agents to bind glass fiber surface to unsaturated polyester matrix.

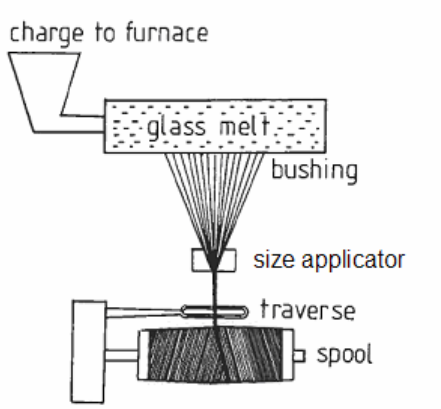

Figure 1.9. Schematic diagram of fiber manufacturing

1.4.2. Organofunctional Silanes

Silane chemistry and its interaction with both glass surface and polymer resins have been studied extensively. Silane coupling agent is used for improving the bond quality and it has first appeared in the literature with the work of Rochow in 1951 [10]. Then a wide variety of organofunctional silanes has been developed, prominently by Plueddemann and coworkers (1962).

Silane coupling agents have the ability to form a durable bond between organic and inorganic materials. They are molecules that have both organofunctional groups and hydrolyzable groups attached to a silicone atom. Silanes bind to the matrix material from organofunctional group and they bind to the glass from hydrolyzable group. By this way an organic material can be chemically bonded to an inorganic surface [11].

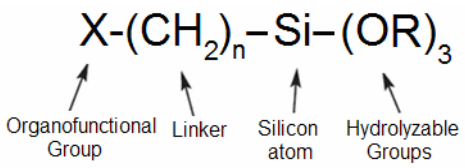

Figure 1.10. General formula of organofunctional silanes

Figure 1.10 shows the general formula of silanes. For fibers that are designed to reinforce unsaturated polyesters, X represents the organofunctional group which contains double bond or amine functionality. Vinyl, hydroxy, thio, epoxy, acrylate, methacrylate, carboxy, amine, alkyl and ester substituted silanes in particular have been established wide commercial applications for polyester resin composites today. OR represents the three hydrolyzable groups which give reaction with the silanols on the glass surface. They are usually methoxy or ethoxy groups.

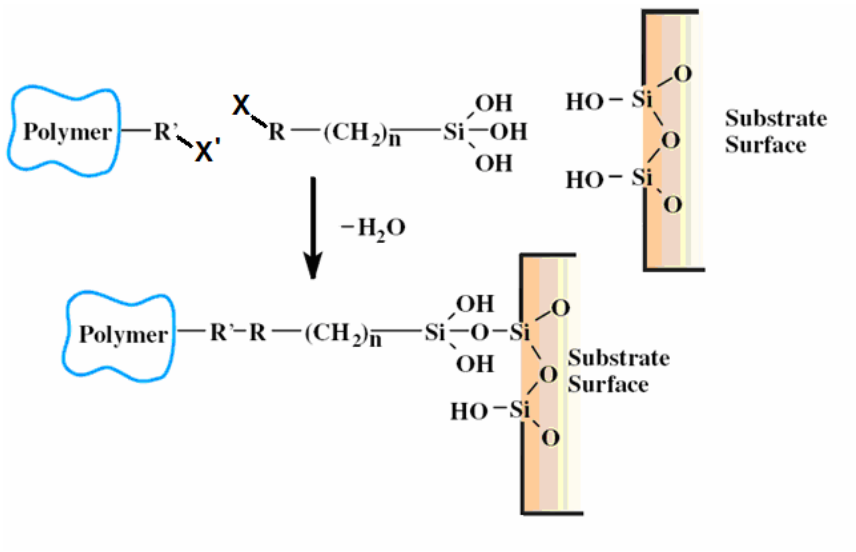

Figure 1.11. Representation of binding process of polymer to glass fiber surface by the help of silane

Organofunctional silanes are generally used as adhesion promoters/coupling agents, surface modifiers and crosslinking agents [12]. As coupling agents, organofunctional silanes give a reaction which helps to bind the polymer matrix to the surface of glass fiber that is illustrated in Figure 1.11.

Silane coupling agents are critical components of glass-reinforced polymers. The glass is very hydrophilic and attracts water to the interface. Without silane treatment on the glass surface, the bond between the glass fiber and the resin would weaken and eventually fail, making a composite essentially useless.

Once the silane coated glass fiber are in contact with uncured resins, organofuctional groups on the fiber surface react with the functional groups that are in the polymer resin to form a sTable covalent bond with the polymer. It is essential that the organofunctional group on the silane should be chosen so that they can react with the functional groups in the resin under given curing conditions.

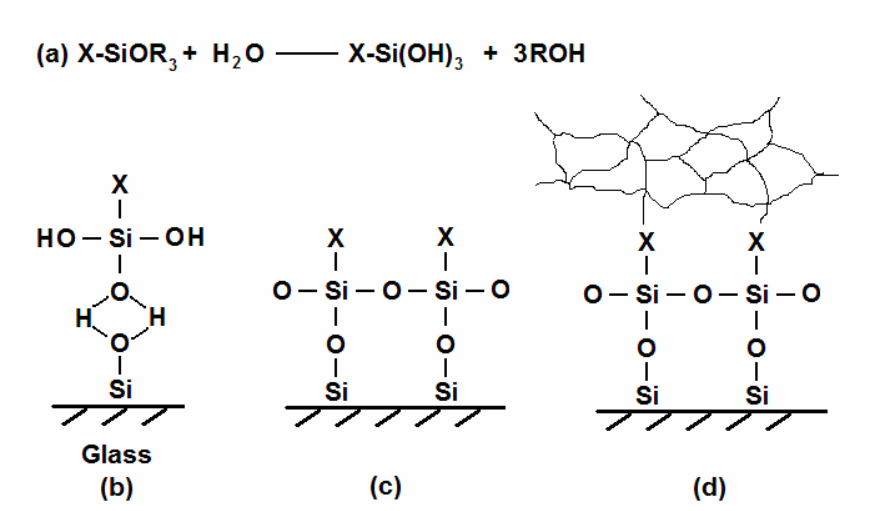

Figure 1.12. Functions of organofunctional silane as a coupling agent

Reaction of the silane with the substrate involves mainly four steps. The first step is the hydrolysis of alkoxy groups (Figure 1.12.a). Upon hydrolysis reactive silanol groups are formed. After hydrolysis step hydrogen bonded silanols between the silanols of the organofunctional silane and the silanols on the surface of glass give condensation reaction to form covalently bonded silyl ethers (Figure 1.12.b, c). During that step water is eliminated. Finally silane binds to polymer by its organofunctional group (Figure 1.12.d). [12]

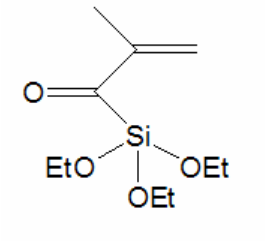

Figure 1.13. Structure of methacryl silane

In general, the effectiveness of the silane as a coupling agent depends on the reactivity of its organofunctional group with the resin. Silane monomers can be also used in integral blends of fillers and liquid resins in the preparation of composites.

Methacryl silanes are used as coupling agents. The glass fiber was prepared by applying on the surface a sizing containing methacryl silane to thereby serve as a reinforcement suiTable for glass FRPs employing as a matrix resin unsaturated polyester resin. That is, methacryl silane improves bonding between the unsaturated polyester resin and the surface of the glass fiber. Thus, the mechanical strength of glass fiber-reinforced thermosetting plastics improves [13]. In Figure 1.13 the structure of methacryl silane is shown.

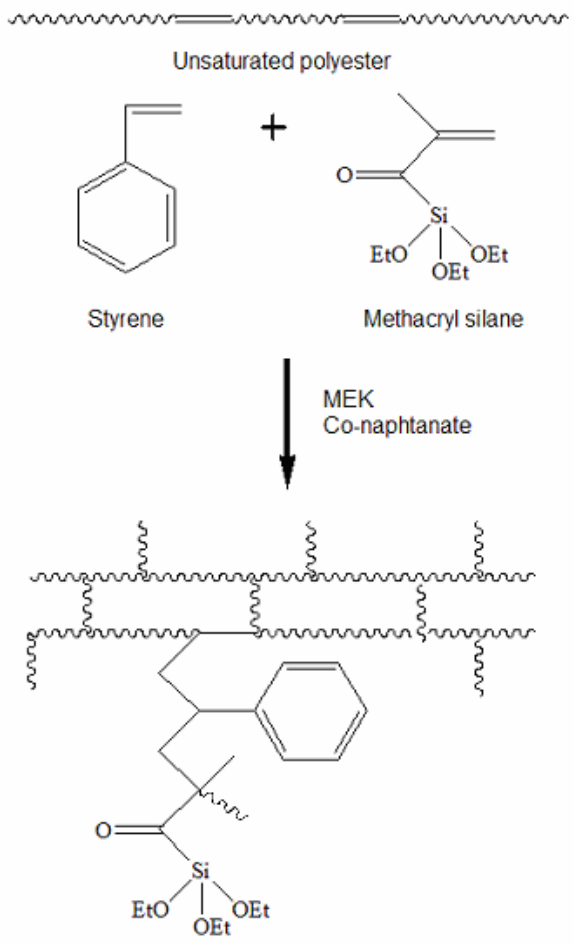

Figure 1.14. Mechanism of the reaction of methacryl silane with unsaturated polyester and styrene

Figure 1.14 shows the reaction mechanism of methacryl silane with unsaturated polyester and styrene. Methacryl silane like styrene reacts by free radical polymerization in

the presence of catalyst MEKP and accelerator cobalt naphthenate. There is no certain sequence for styrene and methacryl silane for aligning on the crosslink.

Aminosilanes are another type of organofunctional silanes, which have amine functionality as organofunctional group. Amine can be primary, secondary or tertiary. The most widely used aminosilane is 3-Aminopropyltriethoxysilane which is represented in Figure 1.15.

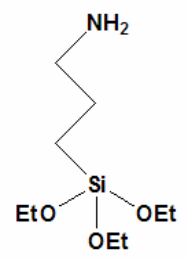

Figure 1.15. Structure of 3-Aminopropyltriethoxysilane

3- Aminopropyltriethoxy silane has two functional groups. Silicon functional group can hydrolyze in the presence of water to the corresponding reactive silanol and organophilic amino group can bind to the polymer with the amine functionality.

In the case of unsaturated polyester, aminosilanes can be added to maleic double bonds by Michael addition reaction. Michael addition is 1,4- addition of a nucleophile to α, β- unsaturated carbonyl groups. The mechanism goes through the addition of aminosilane to the α, β- unsaturated carbonyl group of maleic acid to give an intermediate, enolate.

Figure 1.16 shows the Michael addition of 3-Aminopropyltriethoxysilane to maleic double bonds. There are two β carbons on the maleate. The attack of aminosilane is not stereospecific. So the final product is a mixture of Michael addition of aminosilane to the both β carbons.

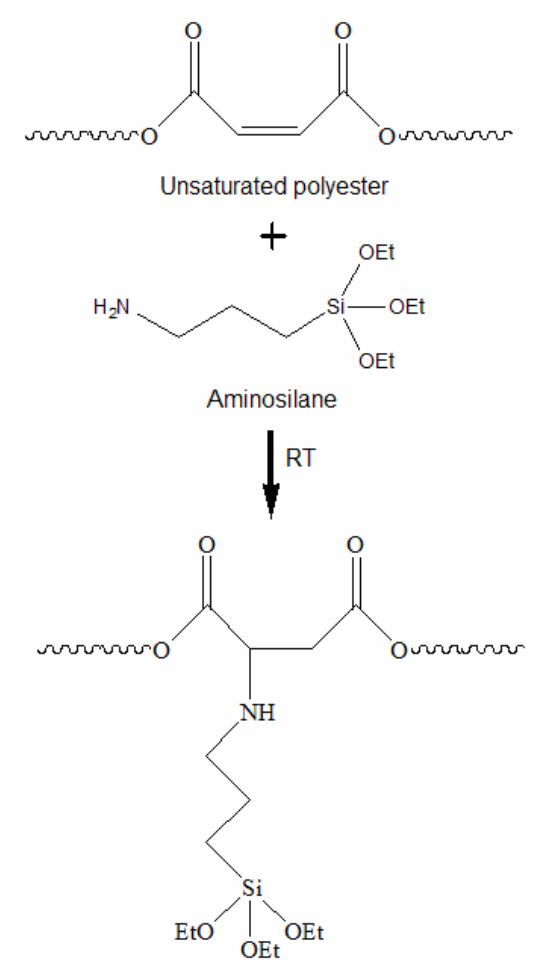

Figure 1.16. Mechanism of Michael addition of amino silane to unsaturated polyester

1.5. Evaluation of Interfacial Adhesive Strength

Measurements of interfacial properties must be conducted in order to evaluate mechanics models or to empirically correlate composite behavior with the interface properties [14, 15].

In industry, composite performance is generally assessed by macroscopic tests that measure composite tensile strength. Composites, unlike metals, are a construction of fibers,

matrix and an interface that is not formed until the composite is manufactured. Due to the heterogeneous nature of composites, the strength and failure characteristics are controlled by many factors. These factors are: fiber type, resin type and degree of cure, fiber architecture, fiber volume fraction, fiber misalignment, void content, fiber-matrix interface properties, and localized composite stresses [16]. For example due to the voids between the fibers, the experimentally measured density of a composite sample is always less than the calculated one. Therefore macromechanical test results reflect the combined effects of processing conditions and constituent properties. As a result, composite optimization proceeds by a trial and error approach and macromechanical tests always involve unacceptably high data spread. As such they are totally inadequate in evaluating different sizing compositions on glass fiber.

As an alternative to this approach, researchers have attempted to use micromechanical tests to predict the performance of a composite from its constituent materials.

1.6. Micromechanical Test with Single Fiber

Since the fiber-matrix interface is not formed until the manufacturing process, a fast, inexpensive, and accurate method of assessing the properties of the fiber-matrix interface has been sought to facilitate this process. These tests involve the use of a single fiber and they represent a perfectly wetted and perfectly void free interface. With such micromechanical tests, the only variable is the interfacial adhesive strength therefore effects of different sizing compositions on the glass fiber can be evaluated.

Micromechanical tests have a variety of specimen geometries and scales involved. In these tests, the bond quality at the fiber-matrix interface is measured in terms of the interface fracture toughness, G_{ic}, or the interface shear (bond) strength (IFSS), τ_b, for the bonded interface. Also the interface frictional strength, τ_{fr}, which is a function of the coefficient of friction, μ, and residual fiber clamping stress, q_0, is measured for the

debonded interface. Therefore, these tests are considered to provide measurements of the interface properties relative to the test methods based on bulk composite specimens. In the following sections, the microbond, the microindentation and the single fiber fragmentation tests are explained.

1.6.1. Microbond Test

Microbond test method is a variation of the fiber pull-out test for polymer composites [17,18]. In the single fiber microbond test, resin is sprayed into spherical droplets on a single fiber and cured. The droplets normally form concentrically around the fiber in the shape of ellipsoids and retain their shape after curing. One end of each fiber specimen is glued to a metal tab which can be connected to a load cell. The droplet is gripped with a micro-vise which is mounted on the crosshead of the tester. The fiber specimen is then pulled out of the droplets between micro-vise until the failure starts, while restraining the matrix and the force to move the droplet is measured. The process is very similar to the act of pulling the skewer out of a shish kebab. This method is illustrated in the Figure 1.17.

The process of having the fiber pulled out from the matrix is observed to demonstrate several typical stages; fiber debonding, postdebonding friction of fiber against debonded surfaces, and finally, either the fiber breaking or fiber being pulled out by the matrix.

A common interpretation of these tests is to reduce the load at failure to an interfacial shear strength (IFSS) by dividing the applied load by the total interfacial area. Physically this term is the average interfacial shear stress at the time of failure. ISS has some use in qualitative work; it is less useful for fundamental characterization of the interface. It also requires the measurement of forces of a few dynes.

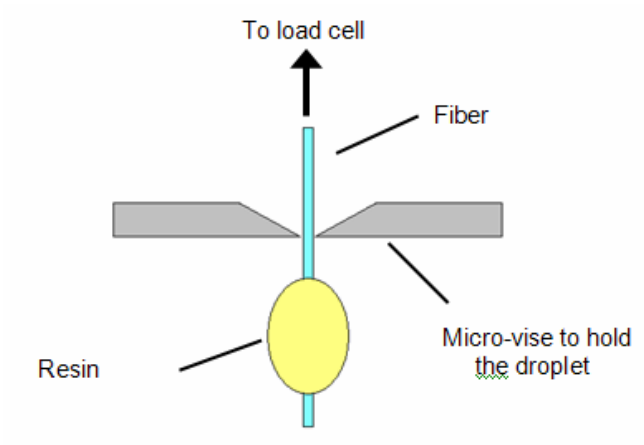

Figure 1.17. A microbond test method

1.6.2. Microindentation Test

A Vickers indentation instrument was used by Marshall [19,20] to exert an axial force on fibers in a polished section cut normal to the fiber alignment. If the fiber is weakly bonded to the matrix (frictional forces only) the exertion by the diamond tip which is similar to pushing out a skewer from the shish kebab, will result in a compression of the fiber with concomitant axial displacement below the polished section surface over a debonded length. Then the force to move the fiber is measured. This method is illustrated in the Figure 1.18.

The relationship between interface friction stress τ, the force on the indentor P, and the distance μ that the fiber is depressed with respect to the matrix, is given by

$$\tau = P^2 / 4\pi^2 \mu r^3 E_f \qquad (1.1)$$

where r is the fiber radius and E_f is the axial Young's modulus of the fiber.

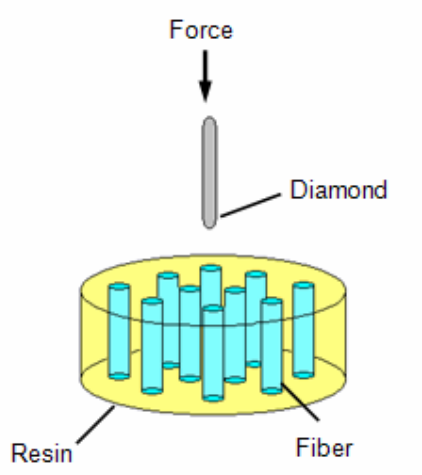

Figure 1.18. A microindentation test method

These tests all require high precision and require the measurement of forces around 1 dyne and movement of 0.1 mm to an accuracy of 1 per cent. Instruments that are capable of doing these tests are quite expensive.

1.7. Background of Single Fiber Fragmentation Test (SFFT)

The fiber matrix interphase can play an important role in the performance of a composite, and consequently, it has been the subject of considerable study. And the single fiber fragmentation test is one of the most popular methods to evaluate the interface properties of FRPs. This test does not involve errors caused by fiber-fiber interactions, void content, and the effect of residual stresses or incomplete cure.

Among the micromechanical testing methods for evaluating fiber-matrix interphase properties of fiber-reinforced composites, the single fiber fragmentation test has attracted special attention since the method was introduced by Kelly and Tyson. The single fiber fragmentation test was originally proposed by Kelly and Tyson [21] for brittle fibers, like tungsten, embedded in a copper matrix. The applicability of this technique for measuring

the interfacial properties of FRP composites has been verified experimentally by Schultz and Nardin [22, 23]. They found that the fiber/matrix shear strength obtained by the single fiber fragmentation test is linearly proportional to the reversible work of adhesion between the two materials for a wide variety of polymer/fiber composites. The fragmentation test is now widely used for measuring the effect of different glass sizing on the interfacial shear strength because of its simplicity in specimen preparation, ease of testing and wealth of information obtained in terms of damage processes [24].

However SFFT is still far from a routine test which is appropriate for industrial applications to examine improvements. Moreover, since SFFT is an indirect method for evaluating the fiber-matrix interfacial properties, a number of micromechanics models have been developed to analyze the fiber fragmentation data based on certain assumptions. In this work SFFT has been modified by simplifying the apparatus, using microscope photography and simplifying the data evaluation to be able to compare the interphases between different fibers and matrix.

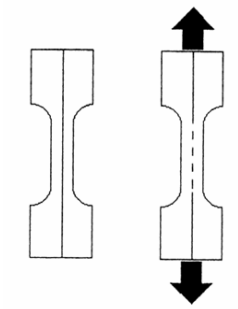

Figure 1.19. Dumbell shaped test specimen

Briefly, in this technique a fiber is embedded in a polymer matrix coupon and a strain is applied to the coupon in the direction of the fiber. With increasing the load the fiber fractures into shorter and shorter fragmentations until the shear stress transfer across the interface is insufficient to cause further fracture of the fiber. Figure 1.19 shows the fragmentation process of a dumbell shaped specimen. Fragmentation of the fiber during the experiment is observed by a conventional optical microscope. Therefore the test requires the matrix to be transparent.

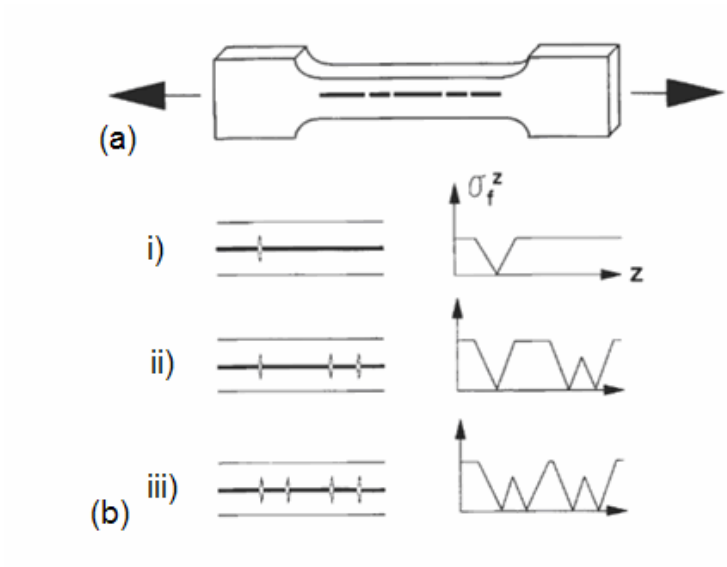

Figure 1.20. (a) Dog-bone shape fiber fragmentation test specimen; (b) fiber fragmentation under progressively increasing load from (i) to (iii) with corresponding fiber axial stress σ^z_f, profile.

Due to the difference in modulus between the rigid glass fiber and the relatively ductile polymeric resin, unsaturated polyester, shear forces are generated at the interphase as the coupon is loaded in tension. The elongation at break of the polyester matrix is 2 per cent while that of the glass fiber is 0.1 per cent. Therefore the test is carried out without breaking the coupon.

If there is a reasonable adhesion between the fiber and the matrix, stress is effectively transferred to the fiber. With sufficient elongation the shear forces exceed the breaking strength of the fiber, causing the fiber to fail within the test coupon. Figure 1.20.(b) illustrates the fiber fragmentation process under progressively increasing strain and the corresponding fiber axial stress profile, σ^z_f, along the axial direction. The shear stress at the fiber-matrix interface is assumed here to be constant along the short fiber length [25]. As the straining process is continued the fiber is rendered into successively higher number of fragments with shorter fragment lengths.

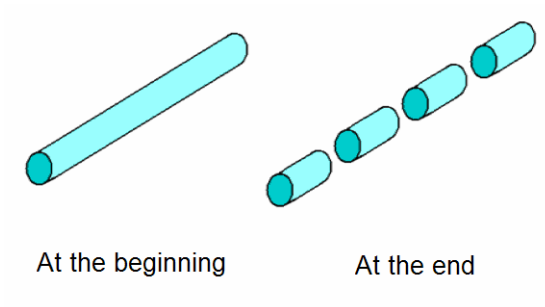

Figure 1.21. The fiber at the beginning and at the end of SFFT

This process continues up to a point where the fiber starts to slide in the matrix. After this point, while the matrix continues to elongate, the fragments do not fragment any longer, since at this point the stress transferred to the fiber is not enough to break the fiber. Figure 1.21 shows the fiber at the beginning and at the end of the fragmentation process. At the beginning of the experiment the fiber is long and has a large surface area. This causes a high stress transfer, so fiber breaks. But when the fiber becomes shorter, it has a small surface area which can not transfer a lot of stress, so that the fiber can not break and slides in the matrix. This point is called as the critical fragmentation point and the average length of fragments obtained is called the critical fragment length. Critical fragmentation point is illustrated as nine fragments in Figure 1.22.

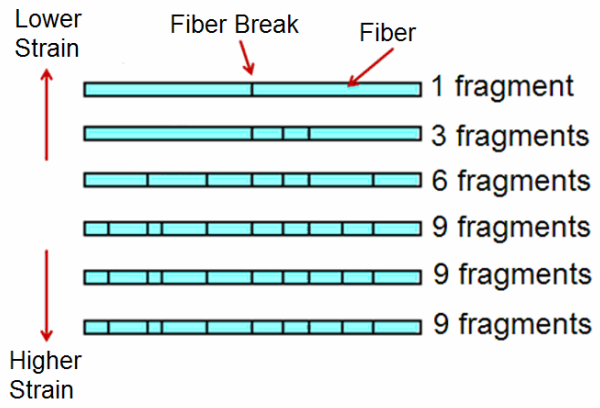

Figure 1.22. Illustration of fragmentation process

The maximum number of the fragments is linearly proportional to the shear adhesion forces that exist between the fiber and the matrix. For example in a system having low bond strength the maximum number of the fragments is lower, as the fiber slides within the coupon.

On the other hand, the number of fiber fragments will be higher in the case of high fiber-matrix interactions because the adhesive forces act more efficiently and translate the shear stress onto the fiber surface. This results in a higher number of breaks. Ultimately a length is reached where no additional fiber fractures can be induced irrespective of the amount of applied strain. This length is the critical length. Expected behavior of a fiber during the loading process is represented in Figure 1.23.

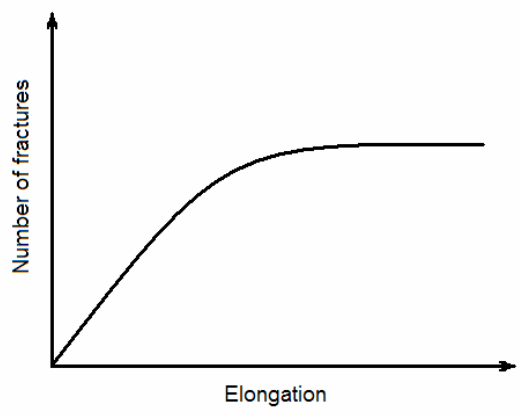

Figure 1.23. Illustration of number of fractures versus elongation graph

The test has the advantage that there is no need to measure any force and any elongation accurately. The test does not measure force at all. It measures only the number of fragments that are produced within a given length of the sample (the gauge length). The strain is however roughly measured so that the experiment is carried out within the elongation limit of the sample. By using a polarizer in the microscope or by adjusting the light intensity the fragments can be easily seen and photographed.

1.8. Multiple Fiber Fragmentation Test

In the literature there is one work where for the purpose of getting more information faster, fiber fragmentation was investigated quantitatively by using multiple fibers instead of a single fiber [26]. The approach of using multiple fiber technique is that it mimics the original composite interphases in a more realistic way than single fiber technique.

In the fragmentation test, the failure process of two fibers which were placed far from each other were examined, and found that the failure profile of the two fibers were similar to the failure profiles from tests done on single fibers. When three fibers were examined, it was found that the measured interfacial shear strength values were much greater than the shear strength values from either the single or two fiber tests. However, when three fibers were used, it was found that it was difficult to control the interfiber spacing. Consequently, whenever the interfiber spacing was too small, breaks in one fiber caused breaks in the adjacent fiber. In conclusion, using multiple fibers in a fragmentation test can not be realistic when the interest is the interphase between the fiber and matrix.

1.9. Observations on Fiber Fracture Modes and Interfacial Debonding Phenomena

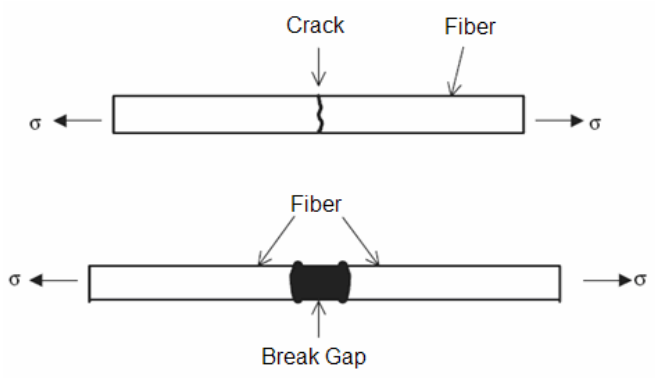

Figure 1.24. Schematic representations of fiber crack and break gap

Tensile fragmentation process starts with a single crack on the fiber and continues with the largening of the crack while the strain increases. At the end break gaps are obtained because the stress transferred to the fiber is not enough to break the fiber fragments any more but causes the fragments slide in the matrix to make the break gap larger. Figure 1.24 shows the initial fiber crack and the break gap at the end of the process.

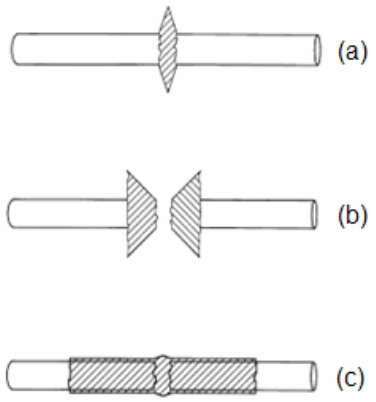

Figure 1.25. The three modes of fracture that arise in a single-fiber composite during a fragmentation experiment.

Regarding the fragmentation configuration, it is known since Mullin et al. [27] that three modes of fracture may arise in a single-fiber composite during a fragmentation experiment, which are based on the degree of interfacial adhesion: (i) In the case of a relatively strong interface, the initial fiber break is followed by a disk-shaped matrix crack, as shown in Figure 1.25 (a). (ii) In the case of a relatively strong interface but with a matrix that has relatively lower shear than tensile strength capability, the initial fiber break is followed by a double cone matrix crack as shown in Figure 1.25 (b). (iii) In the presence of a relatively weaker interface, the initial fiber break is immediately followed by a limited interfacial debonding break as shown in Figure 1.25 (c) [28]. Thus SFFT can give quantitative data in the form of number of fragments over the gauge length, and qualitative data in terms of the matrix cracks and deformation that can be observed under a microscope.

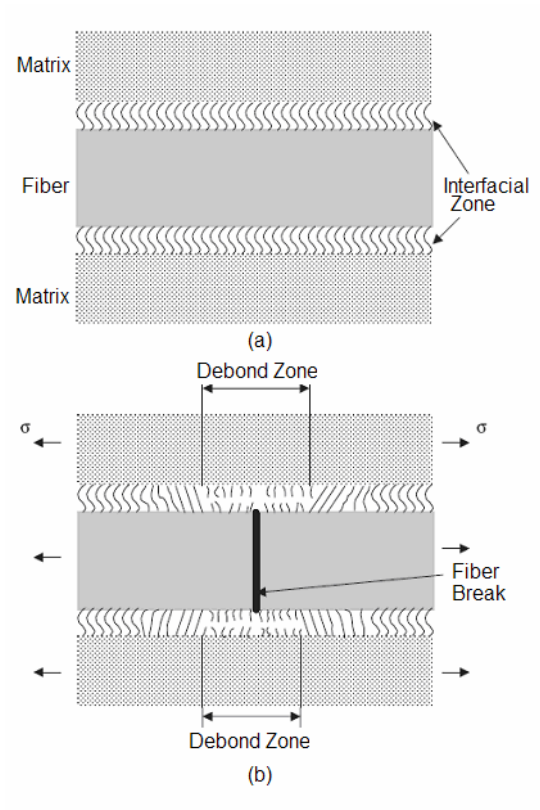

Figure 1.26. Schematic debonding microstructure of fiber and matrix interphase. (a) Before loading (no fiber break); (b) After loading (fiber break).

Debonding phenomena have been investigated as intensively because it is an important part in studying the fracture mechanics of polymer composites. Previous studies show that debonding occurs between the fiber and the matrix when the fiber fails during the tensile loading in composites [29]. When the fiber breaks in single fiber and the polymer matrix debonding occurs simultaneously on the observation time scale as shown in Figure 1.26. Interfacial debonding is a very important property in composites, because composites are composed of different materials and the bonding at the interface can govern the mechanical properties of the composite.

In microscale, the covalent bonds between the matrix and the fiber are broken around the debonding area. This phenomena can be easily observed by using an ordinary optical microscope because the interphase darkens after debonding. This darkening is probably the result of a refractive index change due to local alignment and stress crystallization in the

matrix. The broken bonds causes weakening of the interfacial strength. Fragmentation of the fiber during the loading process is followed by sliding of the fiber around the crack due to the weakened interphase around the crack.

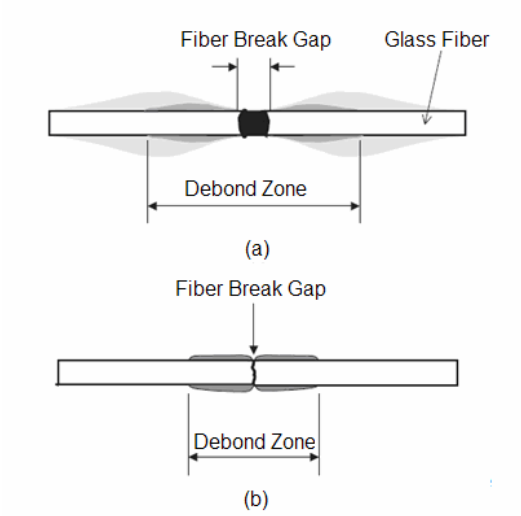

Figure 1.27. Schematic feature of debond zone of E-glass fiber. (a) Loading-applied state; (b) Loading-released state.

As the load application continues, the length of the crack was increased because after cracking process the fiber can slide in the matrix (Figure 1.27.a). If the load was released and time is given to the fiber to slide back to its initial state, it can be observed that the length of the crack is decreased (Figure 1.27.b).

1.10. Atomic Force Microscopic Images of Fiber Surfaces

To simplify fiber-matrix interphase analysis, micromechanical investigations have often modeled the fiber surfaces as homogeneously coated.

A better understanding of fiber surface characterization brings the ability to visualize the wetting of the surface and so interfacial adhesive strength between the fiber and matrix.

Atomic force microscopy (AFM) shows the actual topographic silhouette of surfaces. It also allows inferring interphase properties directly. Among the various techniques utilized, it is originally designed to investigate the material surface properties for various purposes, is an effective and relatively straightforward way to assess interphase characteristics. [30]

The AFM, invented by Binning et al., [31] has become an increasingly popular tool for characterizing surfaces and interphases of many different types of material systems.

The work done by Mäder [32] compared the surfaces of unsized and sized glass fibers. Coupling agents used was γ-aminopropyltriethoxy silane and polyurethane and polypropylene dispersions were used as film formers. It was seen that the surface of unsized glass fiber is relatively neat and simple, but interestingly the surface of sized glass fibers were not homogeneously coated, but size droplets were observed on the surfaces. They characterized the sized fiber surface as size droplets and unsized areas between them. This means size can not totally wet the glass surface, and it can only bind to the matrix from these droplets. This is an important fact that if the wetting ability of the size is high this means there are higher numbers of bonds between the fiber and matrix results higher interfacial adhesive strength.

1.11. Attempts to Improve Interfacial Adhesive Strength Between Glass Fiber and Unsaturated Polyester

As the AFM results of the work which was done by Mäder [32], the adhesive strength can be improved by using the unsized areas on the glass fiber surface. In this work two inventions proposed to increase the number of bonds between the fiber and the matrix by using additional coupling agent beside the one in the sizing. First route is to add methacryl silane directly to the matrix which can be bonded to the matrix from methacryl functionality and to the unsized glass fiber areas from its silane functionality as shown in Figure 1.28.

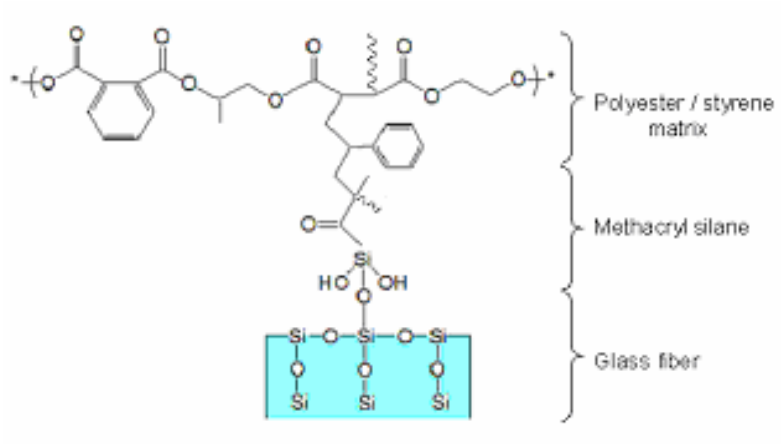

Figure 1.28. Interphase of test sample with methacryl silane added matrix

Second route is to tag a coupling agent to the matrix before the test sample prepared. To achieve this matrix, in the literature Michael addition adduct of an amino organosilane and conjugated unsaturated polyester resin were prepared by Dana and coworkers in 1992 [33]. They adjusted the amount of aminosilane such a way that the unsaturation of the polyester should not be totally consumed, so there should be a considerable amount of double bond at the end of this reaction to be used in the curing process.

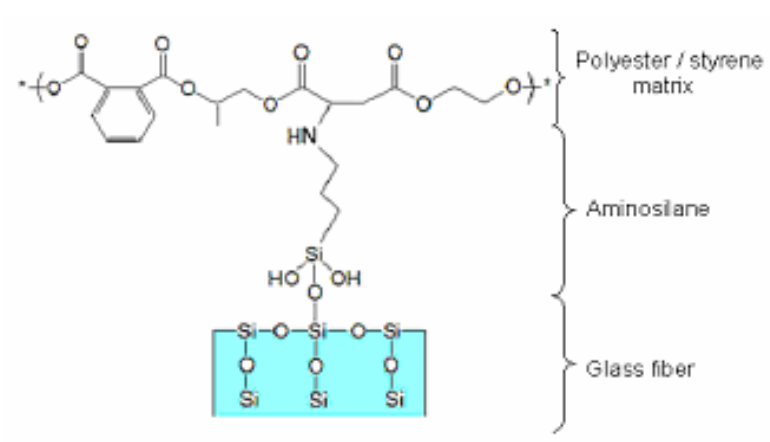

Figure 1.29. Interphase of test sample with Michael adduct of aminosilane and polyester matrix

The amino organosilane that they used was 3-aminopropyltriethoxysilane and 1-methoxy-2-propanol was used as solvent. This reaction was done at 70ºC around one hour to get amino silylated polyester. In this work the attempt is to bind this amino silylated matrix covalently to matrix polymer and bind it to glass surface from its silane functionality as shown in Figure 1.29.

2. STATEMENT OF THE PROBLEM

The aim of this work is to modify SFFT for industrial applications by developing a new approach based on the usage of maximum number of fragments to compare the quality of the interphases for FRP composites. In the literature, computational models were developed to characterize the interphase between fiber and matrix. These models used the critical fragment length that is not useful for industrial applications. Simply counting the maximum number of the fragments would provide a fast and practical test for determining the suitability of the fiber size for a given matrix. This test in its practical abbreviated form would be very useful for a glass fiber manufacturer who is constantly trying to improve the interfacial adhesion by the choice of better sizing formulations.

AFM images will be examined to see if unsized areas on the surface of the glass fiber exist. These areas will be used to increase the adhesive strength between fiber and matrix by using two methods of introducing a coupling agent into the interphase. First method is to add methacryl silane to CE-92 directly and then cure in the sample mold. Second method is to bind an aminosilane to polyester by Michael addition. The SFFT results will be examined to observe the improvements.

3. RESULTS AND DISCUSSIONS

3.1. Behavior of the fibers during SFFT

Micro-straining test apparatus that fits a standard Zeiss microscope was manufactured as described in the experimental section.

SFFT was applied to the specimens with a filament which is 15 µm in diameter. At each 0,1mm extension, breaks were counted. The behavior of the commercial fibers WR-5 and WR-4 manufactured by Cam Elyaf A.Ş is shown in Figure 3.1.

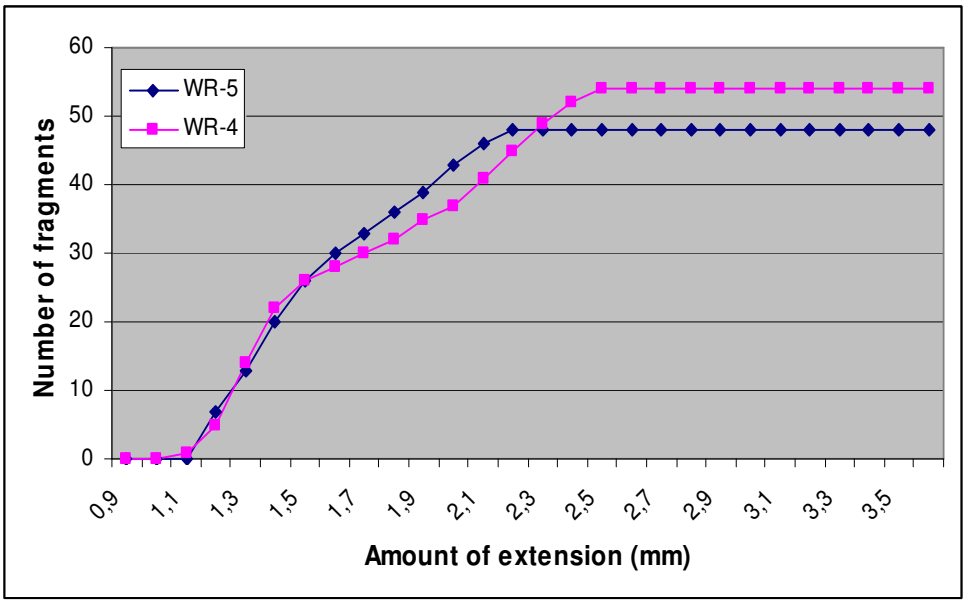

Figure 3.1. Number of fragments as a function of extension for the specimens with WR-5 and WR-4

During the application of the load, the number of the fragments increased at first. Then as the fractures reached the critical length, fiber fracture ceased and the graph reached a plato at the maximum number of fragments. The length of the fragments decreases as the load increases until reaching critical fragment length. Because at that point the load transferred from the matrix to the fiber can not be enough to break the fiber more. If the gauge length is divided by the number of fragmentations, an average number for critical fiber length can also be obtained.

The maximum number of fragment can be used as a measure of the interfacial adhesive strength of the FRPs. For WR-5 and WR-4, eight specimens tested and Q-test was applied to the maximums and minimums of each set of data for 90% confidence level. The ratio (Q_{exp}) of the difference between the tested data and the data nearest to that data and the difference between the maximum and the minimum data was calculated. Q_{crit} value for 90% confidence is 0.47 for eight data. If Q_{exp} was lower than Q_{crit} the data was retained. If Q_{exp} was higher than Q_{crit} the data was rejected. With the retained data, the averages were calculated for WR-5 and WR-4 and found as 48.00 and 54.00 respectively. The specimen with WR-4 fiber which gave higher value of maximum number of fragment has better interphase quality than the specimen with WR-5 fibers. [34]

3.2. Comparing SFFT results with the Macromechanical test results

SFFT was applied to the specimens with WR-5, WR-4, and WR-3. All those fibers are made of E-glass, but they have different coupling agents and different sizing chemistry. The averages of the maximum number of fragments were calculated for WR-5, WR-4, and WR-3 as explained in Section 3.1 and found as 48.00, 54.00, and 59.60 respectively which are shown in Figure 3.2.

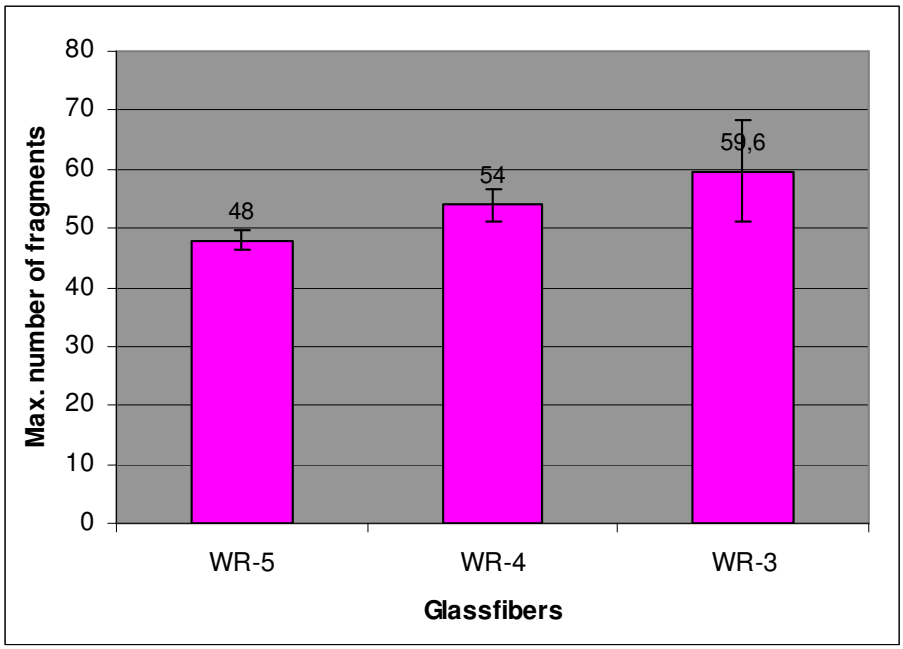

Figure 3.2. SFFT results: Maximum numbers of fragments for WR-5, WR-4, and WR-3

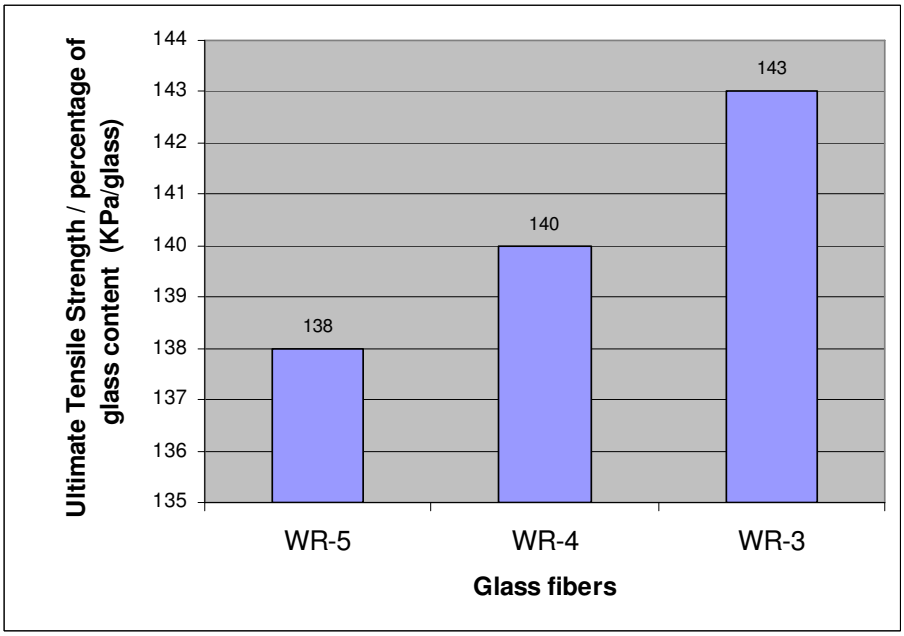

Figure 3.3. Macromechanical test results: Normalized ultimate tensile strength of WR-5, WR-4, and WR-3 per glass per cent.

The same fibers and matrix combination were used to make large ASTM test samples and were separately tested at Cam Elyaf A.Ş. by using standard macromechanical tests. The ultimate tensile strength over percentage of glass content values for 1200 tex WR-5, WR-4, and WR-3 are 138, 140 and 143 KPa / %glass respectively.

In order to prove the reliability of SFFT, the results were compared with the macromechanical test results which were carried out by Cam-Elyaf A.Ş. Macromechanical results for 410, 1200 and 2400 tex strands of WR-5, WR-4 and WR-3 are shown in Table 3.1 together. Tex is a unit of thickness for a fiber strand defined as the weight of 1000 meter strand in grams. The values for maximum tensile strength normalized to per unit of glass fiber. This normalization is required because there are always small errors in the fiber content of the macromechanical test sample.

Table 3.1. Macromechanical test for the samples with WR-5, WR-4 and WR-3

Fiber	**Macromechanical test results**		
	410 tex (KPa/glass)	**1200 tex (KPa/glass)**	**2400 tex (KPa/glass)**
WR-5	87	138	124
WR-4	120	140	141
WR-3		143	

To calculate the percent improvement from WR-4 to WR-5, each WR-5 data were subtracted from WR-4 data, then divided to WR-5 values and multiplied by hundred. The average of the improvements for macromechanical test results and SFFT results were found as 17.70 and 12.50 per cent respectively. If the macromechanical test results are supposed to be a reference, it was observed that SFFT results are accurate. But the fluctuation of the results for different tex strands obtained by using macromechanical test shows that there are some errors in the test and this shows the limits of confidence of the macromechanical

test results are low. It should be noted that higher tex strands include more fibers and wetting of fibers in high tex strands by the liquid resin is more difficult.

Table 3.2 compares the improvement percentages between the macromechanical tests and SFFT. The values found by using macromechanical test for the specimen with WR-3 fiber are higher than for the one with WR-4 fiber and WR-5 fiber, this result is also found by SFFT. But the percentages resulted by SFFT are higher than percentages resulted by macromechanical tests. This proves SFFT can measure the smaller improvements better than macromechanical tests. Because a lot of errors can be eliminated by SFFT.

Table 3.2. Comparison of macromechanical test and SFFT results for the samples with WR-5, WR-4 and WR-3

Fiber	Macromechanical test results 1200 tex (KPa/glass)	SFFT Results
WR-5	138	48.00
WR-4	140	54.00
WR-3	143	59.60
Improvement achieved by WR-4 (%)	**1.44**	**12.50**
Improvement achieved by WR-3 (%)	**3.62**	**24.17**

SFFT proved to be a precise, easy and cheap method to compare interfacial adhesive strengths between glass fibers and polymers for industrial applications. The absolute value of the adhesion strength can not be determined, but different fibers can be compared with good precision.

As a summary, this method with this modification has a lot of advantages like:

- Reproducibility is very good,
- No errors due to imperfection in the sample preparation,
- Easy to observe fragments under microscope,
- Short time is needed for sample preparation and for testing,
- No force measurement,
- No elongation measurement,
- Fiber can totally wet with the polymer,
- No irregularities exist in the sample,
- Results are independent of fiber ratio of the composite.

But there are also two disadvantages of SFFT:

- Difficulty in sample preparation, but this can be easily eliminated by practicing,
- Matrix has to be transparent to be able to observe and count the breaks under microscope.

3.3. Results for other commercial fibers

SFFT was applied to the specimens with 1200 Tex glass fibers obtained from Pittssburg Plate Glass (PPG), Vetrotex (VT), and Cam Elyaf A.Ş. (WR-5). These companies are the world's leading glass fiber manufacturers. They were E-glass but they had different coupling agents in the sizing. The purpose was to demonstrate that SFFT could distinguish between these fibers in terms of interfacial strength. Figure 3.4 shows the maximum number of fragments and they were found to be 43.00, 51.42 and 65.20 for WR-5, PPG and VT respectively. WR-5 had the lowest value between them; this means that the specimen with WR-5 fiber has the lowest interphase quality.

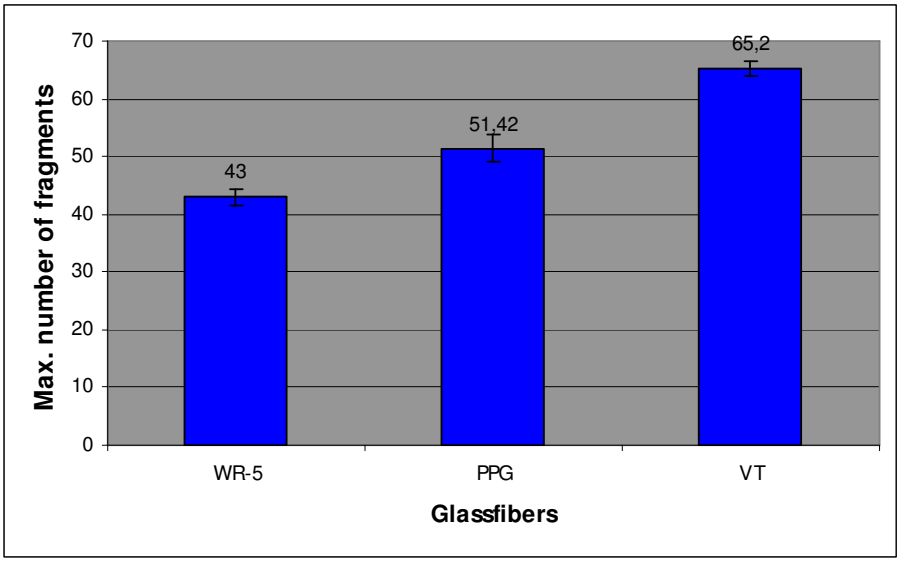

Figure 3.4. SFFT results: Maximum number of fragments for PPG, VT, and WR-5

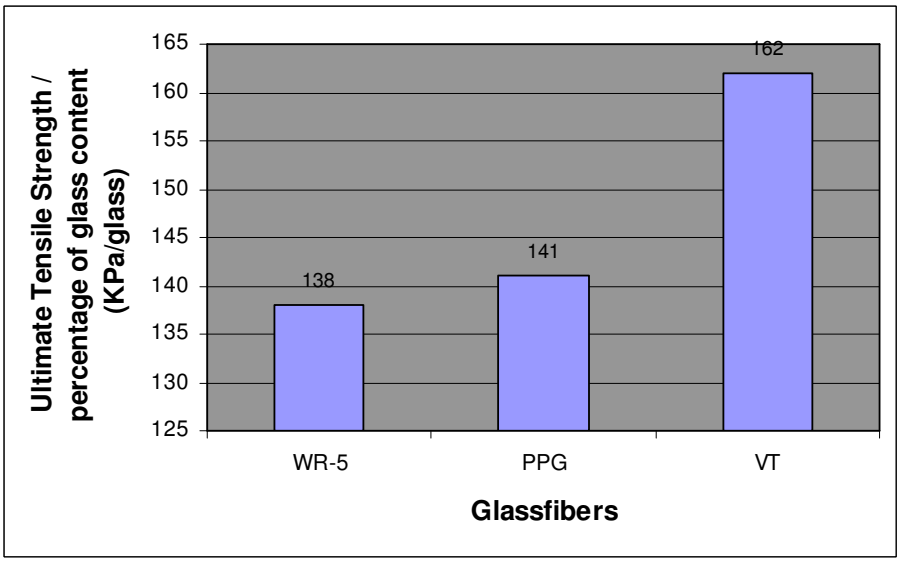

Figure 3.5. Macromechanical test results: Normalized ultimate tensile strength for 1200 tex WR-5, PPG and VT

Macromechanical test results were found to be similar to SFFT results. Figure 3.5 shows the macromechanical test results taken from Cam-Elyaf A.Ş. The maximum tensile strengths which were normalized to per unit of glass fiber were found to be 138, 141 KPa/glass and 162 KPa/glass for WR-5, PPG and VT respectively by macromechanical test. The adhesive strength for the specimen with VT is better than the others as a result of macromechanical test. Also as SFFT results, VT had the highest number of fragments, so it had better adhesive strength than PPG.

3.4. Results for Unsized and Improperly Sized Fibers

SFFT was applied to the specimens with 1200 tex glass fiber with sizing optimized for polypropylene resin (PP), unsized glass fiber (unsized GF), and WR-5. It is expected that when PP fiber which has a sizing suiTable for polypropylene is used with a polyester matrix, SFFT should show a very low interfacial strength. Also a fiber with no sizing should have low interfacial adhesion. WR-5 which has a sizing optimized for polyester should show a high interfacial adhesion.

Figure 3.6 shows the maximum number of fragments found as 9.52, 12.60, and 48.25 for unsized GF, PP and WR-5 respectively. Because coupling agents were applied to glass fibers to make them bonded to the matrix covalently, this result is the expected behavior for unsized glass fiber was having the smallest fragment number, due to no adhesive strength at the interphase. This behavior can be explained as unsized glass fiber in uncoated to make it bonded to the matrix. So it can easily slide in the matrix. It should not be broken in the matrix, but when unsized glass fiber was handled, it was observed that it was easily broken and it had static electricity. These can make the failure of the fiber in the test sample.

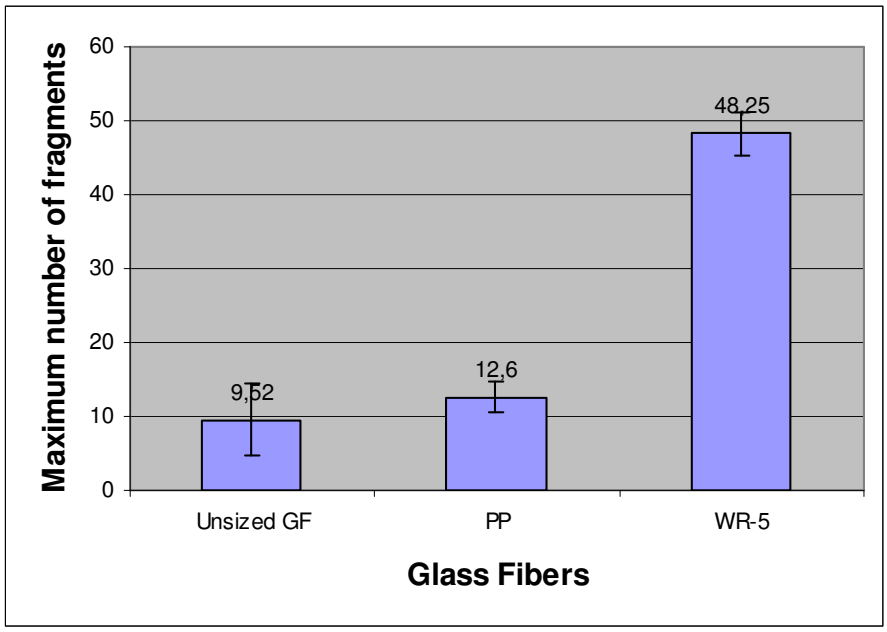

Figure 3.6. SFFT results: Maximum number of fragments for unsized GF, PP and WR-5

On the other hand PP which was coated with sizing which included a coupling agent designed for polypropylene resin can not make any covalent bond with polyester resin. Thus the maximum number of fragments of PP was lower than that of WR-5.

3.5. Observation of different modes of fractures and debonding phenomena

Fracturing process during SFFT was monitored by a digital camera for the specimen with WR-5. Figure 3.9 shows the pictures taken during the test. Figure 3.7 (a) shows a part of fiber WR-5 at the beginning of the process. It has no fragments. Figure 3.7 (b) shows the same part of the fiber in the middle of the process with two fractures and Figure 3.7 (c) shows the same fractures but with longer gap. Because through the end of the process the load transferred to the fiber fragment can not be enough to break it more, so the cracks got bigger without any fracturing.

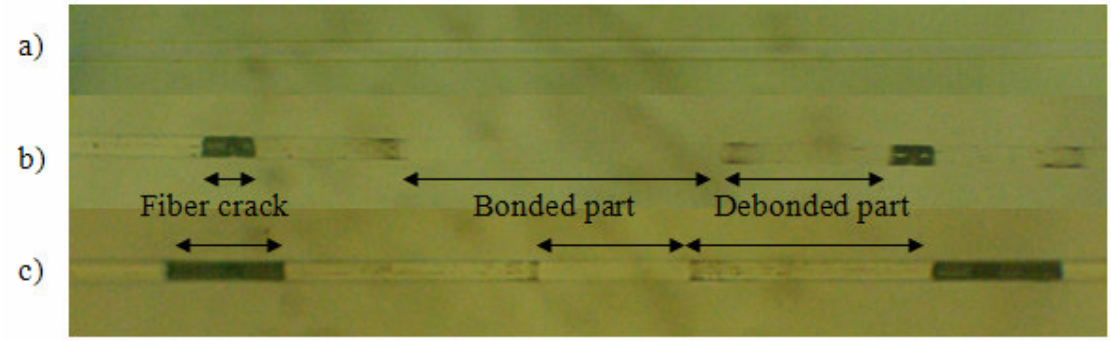

Figure 3.7. Fragmentation process of the specimen with WR-5, (a) at the beginning of the process, (b) in the middle of the process, (c) at the end of the process

The mode of cracks can be different for different fibers depending on the bond quality between the fiber surface and the matrix. It can also be different at different positions along the length of the same fiber.

Different modes of fracture for WR-5 were observed during SFFT. Figure 3.10 shows photographs of the two modes of cracks taken from one fiber during the test. Interface qualities can be considered as a<b. Because in the presence of relatively weak interphase, initial small fiber break is followed by debonding crack. In Figure 3.8 (a) the fiber crack was followed by debonding due to the weakness of the bond between fiber and matrix. In Figure 3.8 (b) because the interfacial adhesive strength is very strong, the bond did not want to break and caused the matrix to crack. We see that SFFT coupled with microscopy allows us to get qualitative data on the fracture mode of the matrix also.

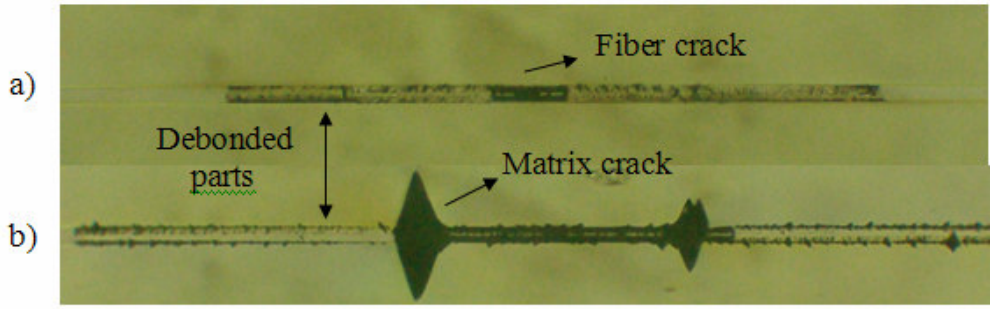

Figure 3.8. Different fragment modes of WR-5

As mentioned before in Section 3.2 WR-5 has the weakest, whereas WR-3 has the strongest adhesive strength. When the fragmentation modes are examined, it was observed that the crack pattern of WR-5 was like in Figure 3.8 (a), and the crack pattern of WR-3 had mostly matrix cracks like in Figure 3.8 (b).

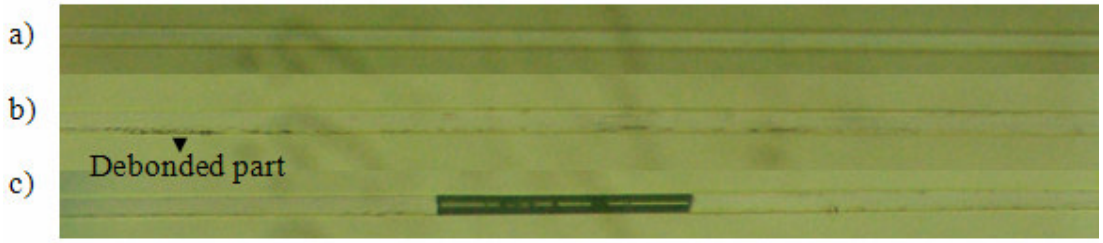

Figure 3.9. Fragmentation process for PP

Debonding around the fiber is not always observed after fiber crack. If the bond is very weak like in the case of PP sample which has a size optimized for polypropylene matrix, debonding between two phases can be immediately seen after very small load application as seen in Figure 3.9 (b). Also as mentioned before, the maximum number of the fragment is very small for this sample. The fiber cracks are very long because the fiber fragments can easily slide in the matrix, and there is no evidence of matrix cracks due to the low interfacial strength.

3.6. Multiple fiber fragmentation test results

For WR-5 and WR-3 two and single fiber included test samples were prepared at the same time. As shown in Figure 3.10 as a result of WR-5 sample with single fiber gave 47.6 fragments where as WR-5 sample with two fibers gave 24.3 fragments at the end of the test. Also WR-3 sample with single fiber gave 55 fragments with single fiber where as WR-3 sample with two fibers gave 20 fragments at the end of the test. Normally WR-3 sample gave higher number of fragments according to SFFT and macromechanical tests. But with more than two fibers they gave unexpected results. This can be explained in this

way: when there is more than one fiber, there are voids between the fibers and the interfiber spacing is difficult to control.

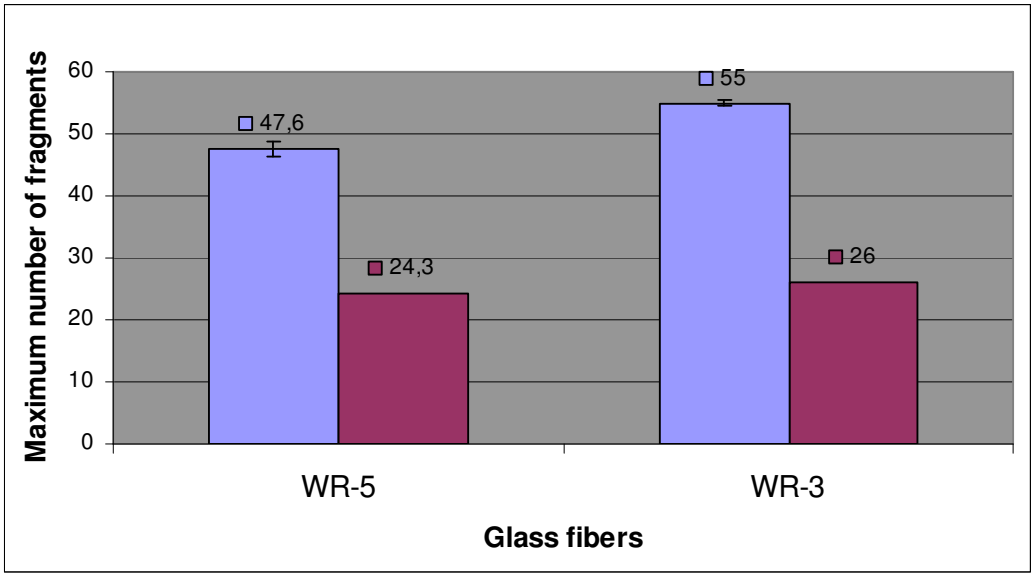

Figure 3.10. Comparison of single fiber and multifiber fragmentation test results.

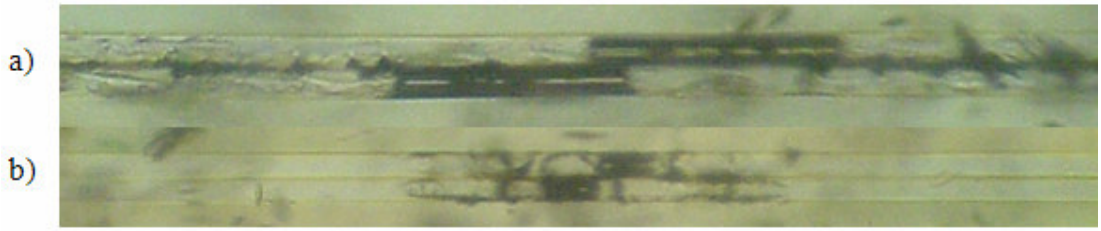

Figure 3.11. Multifiber test samples: (a) WR-5, (b) WR-3

At the beginning all the stress transferred to the fibers from the matrix was equally shared by two fibers. When one fiber is broken, this caused more stress on the second one and it was broken too, but near to the break gap of the first one. This can be easily seen in Figure 3.13. Figure 3.11 (a) and (b) belong to WR-5 and WR-3 respectively. Break points of the two fibers are at the same point or very close to each other. In conclusion using multiple fibers in a fragmentation test has disadvantages because breaks in one fiber caused breaks in the adjacent fiber. With these results we conclude that the multifiber test results

can not be used to prove the efficiency of the fragmentation test.

3.7. AFM results

The atomic force microscope (AFM) is one of the most powerful tools for determining the surface topography of materials. In an AFM a constant force is maintained between the probe and sample while the cantilever tip is raster scanned across the surface. By monitoring the motion of the cantilever tip as it is scanned across the surface, a three dimensional image of the surface is constructed. Figure 3.12 illustrates the scanning process of atomic force microscopy.

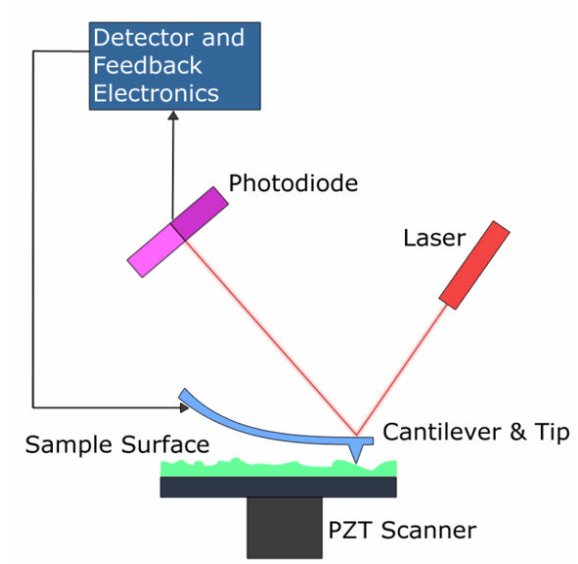

Figure 3.12. Illustration for the scanning process of AFM

In this work to get information about the surface of unsized and sized glass fiber, phase mode imaging was performed using a silicone nitride cantilever probe with a nominal resonance frequency around 170 kHz and a nominal tip radius of 5-10 nm. The topographic images of unsized and sized glass fiber surfaces as shown in Figure 3.13 were compared.

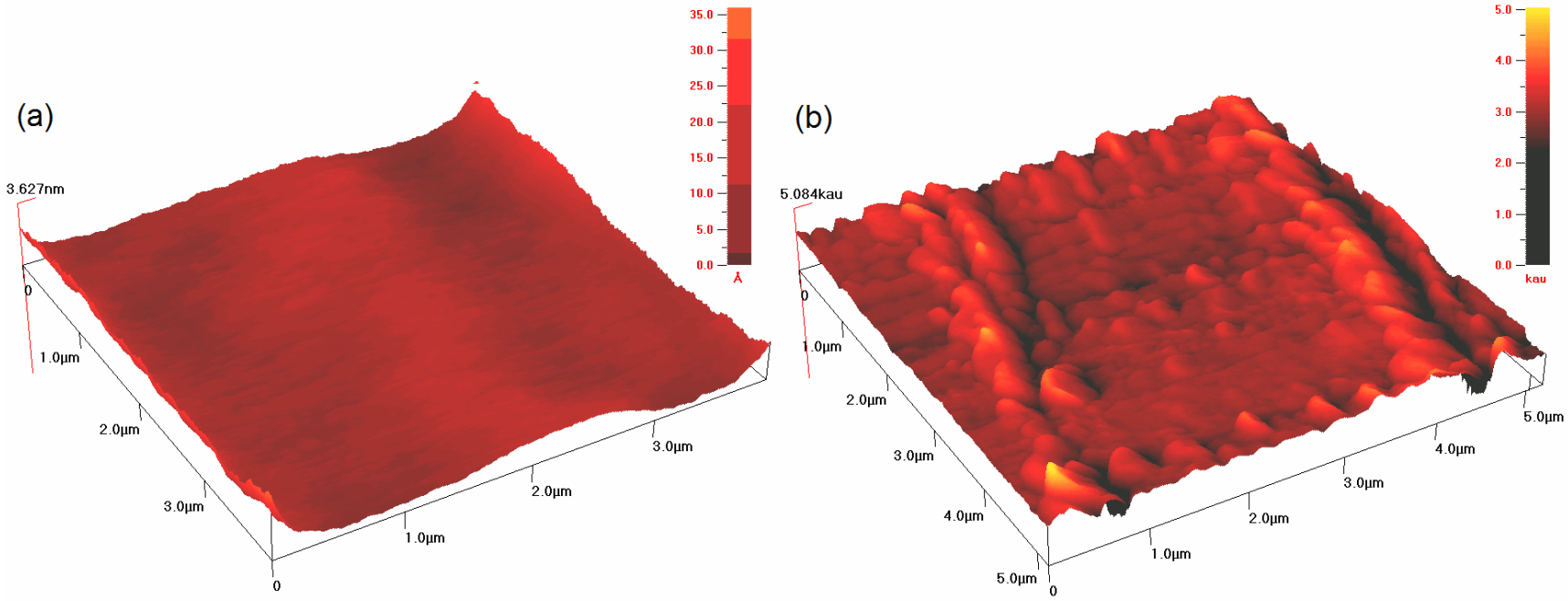

Figure 3.13. AFM image of (a) unsized and (b) sized glass fiber

The surface of unsized glass fiber is flat and uniform whereas the sized glass fiber has sizing droplets on the surface heterogeneously and there are some areas on the surface of the glass fiber with no sizing. Based on these AFM images, new improvements were developed to get better interphase adhesive strength by using the unsized areas on the glass fiber surface.

3.8. Methacryl silane addition into matrix mixture

Mechanical properties of fiber reinforced polymer composites can be improved by improving the mechanical properties of matrix or using better reinforcement, or by improving the interfacial adhesion between the reinforcement and the matrix. AFM images gave an idea that there are unsized part on the surface of the glass fibers that can be used to improve the adhesive strength of the glass fiber to the unsaturated polyester because increasing the number of the bond between the fiber and matrix can increase the interphase quality. With this in mind methacryl silane was added to unsaturated polyester-styrene mixture and used to prepare the test samples. The amount of the methacryl silane is very important because a small amount can not be enough to observe meaningful improvement, on the other hand high amount of methacryl silane can change the mechanical properties of the matrix. The disadvantage of this method is that there is no guarantee that the added methacryl silane will go to the interphase region.

3, 5 and 10 per cent (volume/volume) methacryl silane added unsaturated polyester-styrene mixture were prepared and applied to a single fiber at the same time with the matrix without methacryl silane. WR-5 is the name for the matrix prepared without methacryl silane. 3%MS-WR-5, 5%MS-WR-5 and 10%MS-WR-5 are the samples that methacryl silane was added. Figure 3.14 shows the maximum number of fragments at the end of SFFT for WR-5, 3%MS-WR-5 and 5%MS-WR-5.

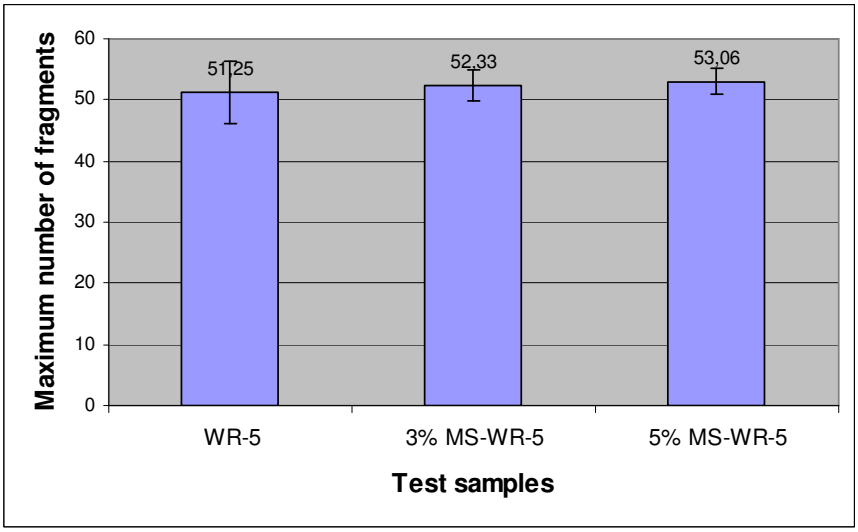

Figure 3.14. SFFT results for WR-5, WR-5 with 3 per cent methacryl silane added polyester, and WR-5 with 5 per cent methacryl silane added polyester

WR-5, 3% MS-WR-5 and 5% MS-WR-5 samples gave the maximum number of fragments of 51.25, 52.33 and 53.06 respectively. The percentages of improvements achieved were calculated by dividing the difference of new samples and WR-5 to WR-5 value. The results are shown in Table 3.3.

It was observed that when the amount of methacryl silane was increased, the interphase quality was increased. But when the sample with 10 per cent methacryl silane added polyester was tested, before the fiber came to the critical fragmentation number, the matrix was broken. So the mechanical properties of the matrix were decreased by adding methacryl silane.

The per cent improvements are not significant amount achievements. Because there is no sequence for the crosslinking reaction of methacryl silane and styrene with unsaturated polyester, styrenes on the crosslink segments may prevent silanol ends of methacryl silane to see the glass surface, so methacryl silanes can not reach to the glass fiber surface. Also the only bonded methacryl silanes are the ones which are close to the interphase. So the job of methacryl silanes in the bulk of the matrix is only crosslinking of unsaturated polyester.

Table 3.3. Per cent improvement achieved by methacryl silane addition

Sample	SFFT Results	Improvement achieved (%)
WR-5	51.25	
3% MS-WR-5	52.33	2.11
5% MS-WR-5	53.06	3.53

3.9. Michael addition of aminosilane to unsaturated polyester

The maleic double bonds are α, β unsaturated which makes them susceptible towards nucleophilic attack via Michael addition reaction. Amines are good nucleophiles and they can easily attack to α, β unsaturated double bonds.

To achieve an improvement at the interphase of glass fiber- unsaturated polyester composites, the results of AFM images gave the idea of to use the unsized parts to get more bonds between the glass fiber and unsaturated polyester matrix. Aminosilanes are organofunctional silanes that can bind to maleic double bonds within the unsaturated polyester and it can bind to glass surface by silane functionality. Thus it can act as a coupling agent but as a coupling agent that is tagged to the matrix.

In this part of the project to improve the interphase quality the second route was to tag 3-aminopropyltriethoxysilane to maleic double bonds such a way that 2/3 of the total unsaturation was not consumed to be used in curing process. The reaction carried on very dry conditions at room temperature not to hydrolyze the ethoxy groups on the silane.

In order to prove that reaction proceeds only through the Michael addition, CE-92 was reacted with 3-aminopropyltriethoxysilane in 1:1 ratio so that all double bonds were deplated in the reaction. The characterization of the product was done by H^1NMR spectroscopy.

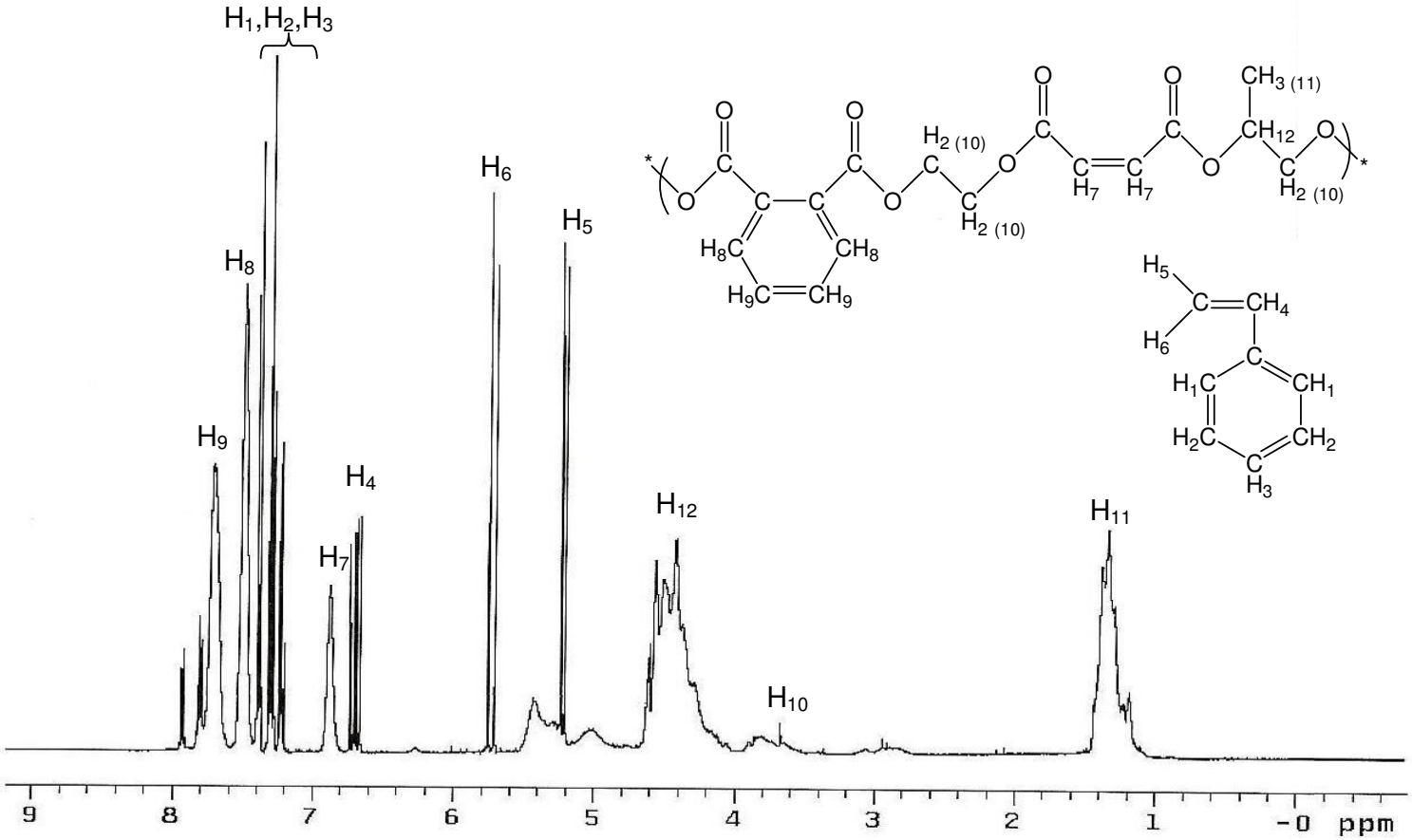

Figure 3.15. ^{1}H NMR spectrum of CE-92

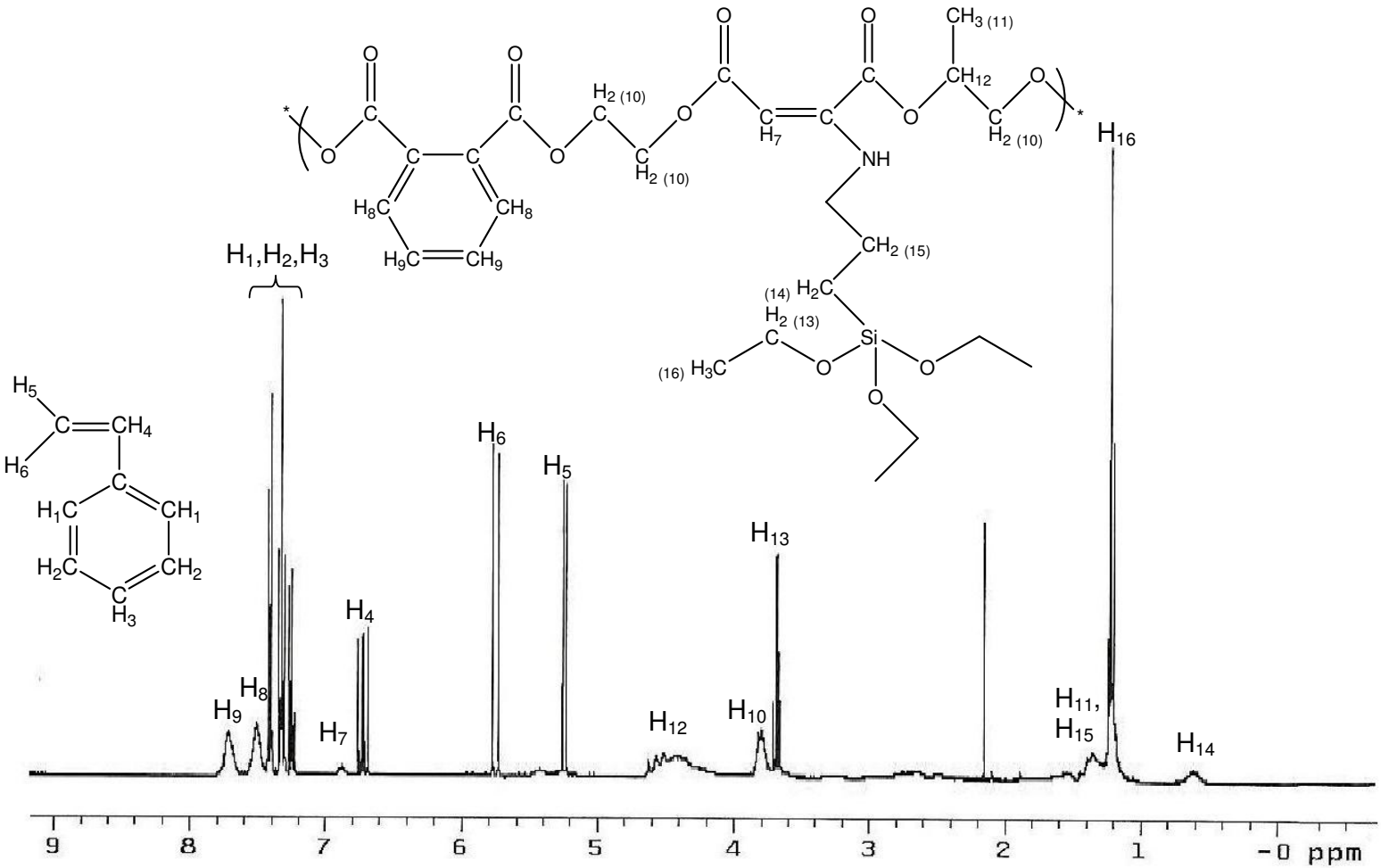

Figure 3.16. . ^{1}H NMR spectrum of 3-aminopropyltriethoxysilylated CE-92

Figure 3.15 is the ^{1}H NMR spectrum of CE-92 and Figure 3.16 is the ^{1}H NMR spectrum of 3-aminopropyltriethoxysilylated CE-92. After the reaction, the decrease in the intensity of the peak at 6.83 ppm, belongs to the protons of maleic double bond, indicates that the reaction proceeds via Michael reaction.

Aminosilylated CE-92 was applied to WR-5 and unsized glass fiber. The sample with WR-5 fiber showed different mode of fragmentation after load was applied compared to the general pattern. As shown in the Figure 3.15, the fragments were continuous with fiber cracks, matrix cracks and debonding part together. The fragments were not distinguishable enough to count. Some part with matrix cracks had no fiber cracks, so the fragments were counted which were been sure that there were fiber cracks. The number of fragments result taken from WR-5 with aminosilylated CE-92 sample is approximate value because of this reason.

Figure 3.15. Picture of WR-5 with aminosilylated CE-92 after the load applied

SFFT results compared with the samples in which the matrix was pure CE-92. For WR-5 / CE-92, WR-5 / CE-92, UGF / CE-92 and UGF / AS-CE-92 SFFT results are 52.75, 65.25, 18 and 11.75 respectively as shown in Figure 3.15. The samples in which aminosilylated polyester was used gave higher number of fragments that proves the improvement on the interphase of the composite.

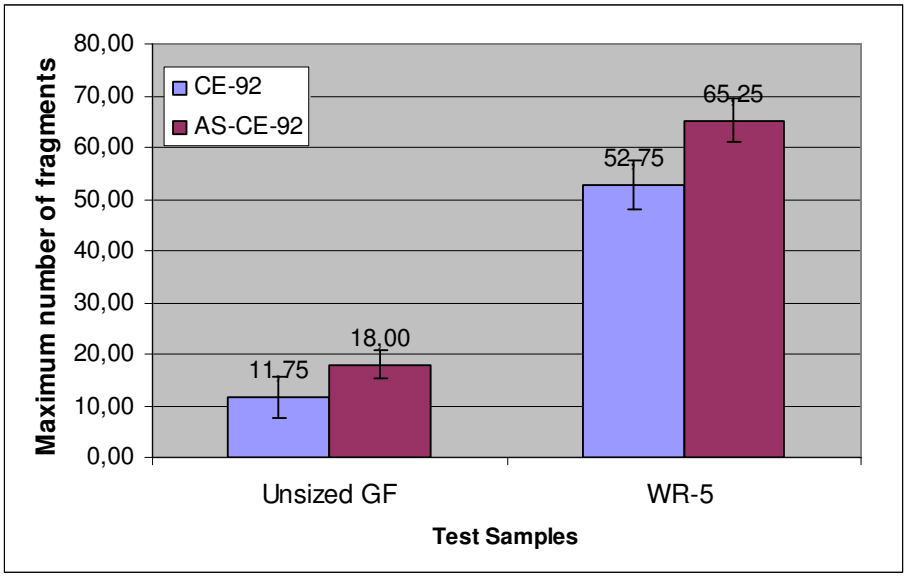

Figure 3.16. SFFT results for Unsized GF and WR-5 with CE-92 and aminosilylated CE-92

Table 3.4 shows the calculated per cent improvements. For WR-5 it was found as 23.70% and for unsized glass fiber it was found as 53.19%. The higher percentage of improvement of the samples prepared with unsized GF is due to the availability of more silanols groups on the surface of the glass fiber.

Table 3.4. Per cent improvement achieved aminosilylated CE-92

Sample	SFFT Results	Improvement achieved (%)
WR-5 / CE-92	52.75	
WR-5 / AS-CE-92	65.25	23.70
UGF / CE-92	11.75	
UGF / AS-CE-92	18	53.19

4. EXPERIMENTAL

4.1. Chemicals and Apparatus

4.1.1. Chemicals

Chemicals that are used in this research are given in Table 4.1.

Table 4.1. Chemicals and suppliers

Chemical	Supplier
Unsaturated polyester-styrene mixture (CE 92)	Cam-Elyaf A.Ş.
Glass fiber strands (1200 tex)	Cam-Elyaf A.Ş.
Methyl ethyl ketone peroxide (MEKP)	Akzo Nobel
Cobalt naphthenate	Akzo Nobel
Methacryl silane	Hüls-Degussa
Amino silane (A1100)	Hüls-Degussa
Hydroquinone	Merck

Unsaturated polyester with brand name of CE 92 was used in this study. It includes 42 per cent styrene as a reactive diluent and it is the product of Cam Elyaf A.Ş. Turkey. Specifications of the resin are given in Table 4.2. This resin is composed of maleic anhydride, phtalic anhydride, ethylene glycol and propylene glycol.

Table 4.2. Properties of UPE CE 92

Specifications	Units	Values
Appearance	----------	Clear
Density	g/cm^2	Min 1,10-Max 1,15
Solid content	%	58
Acid number	Mg KOH/gr	Max 25
Viscosity	cps	Min 340-Max 460
Gelation time	Minute	Min 6-Max 10
Stability	Day	67

Table 4.3. Properties of E-glass fiber

Property	E-glass
Diameter (µm)	5-25
Density (g/cm^3)	2.54
Tensile strength (GPa)	2.4
Elongation at break (%)	3.4
Young's modulus (GPa)	72.4
Coefficient of thermal expansion (10^{-6}/K)	5.0

Glass fibers with brand names of WR-5, WR-4, WR-3, PPG, VT, and also unsized glass fiber and glass fiber sized with a proper coupling agent for polypropylene were used. They are E-glass fibers. WR-5, WR-4, and WR-3 are own products of Cam-Elyaf A.Ş. The properties of E-glass fiber are shown in Table 4.3.

4.1.2. Apparatus

4.1.2.1. Apparatus for Sample Preparation.

- Aluminum foil
- Scissors
- Picks
- Tweezers
- 100ml beaker
- Disposable dropper
- Ruler
- Glass stirring rod
- A silicone mold with eight dumbell shaped cavity

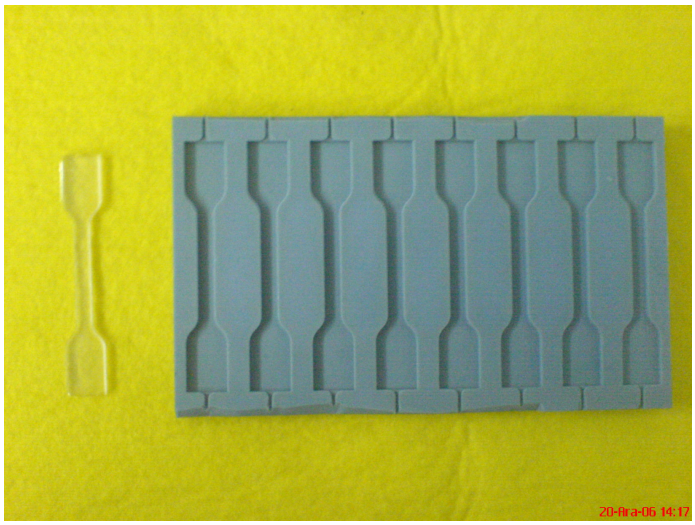

Figure 4.1. The silicone mold with eight dumbell shaped cavity

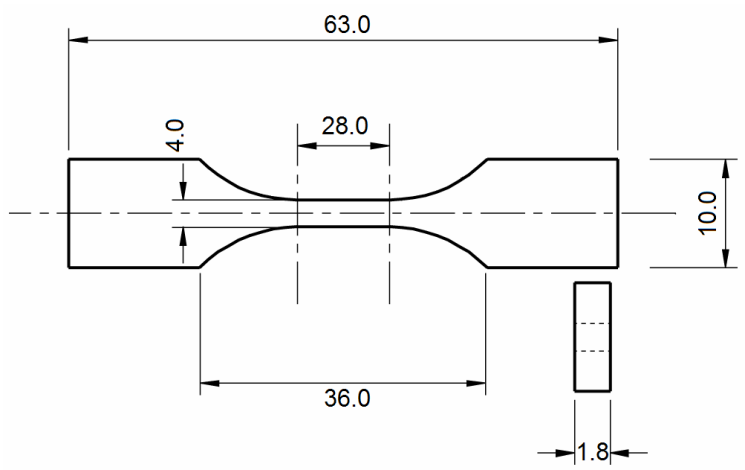

Figure 4.2. Dimensions of dumbell shaped specimen

4.1.2.2. Apparatus for Testing.

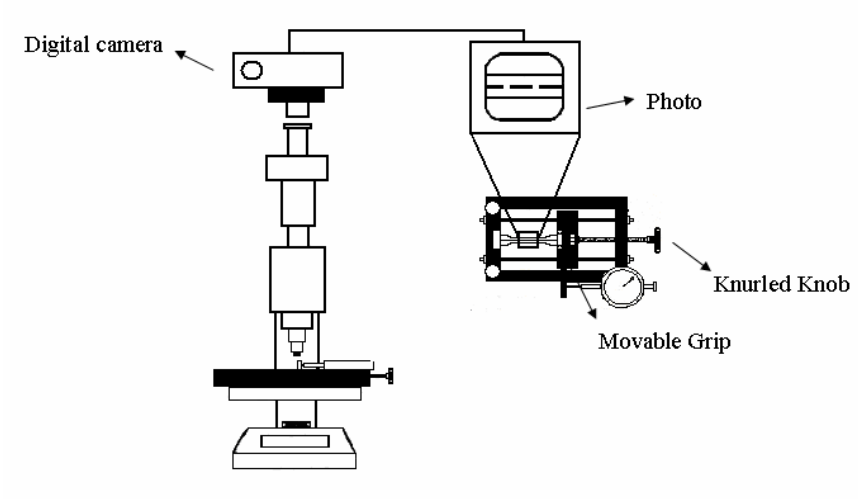

Figure 4.3. Schematic illustration for testing system

- Micro-straining device

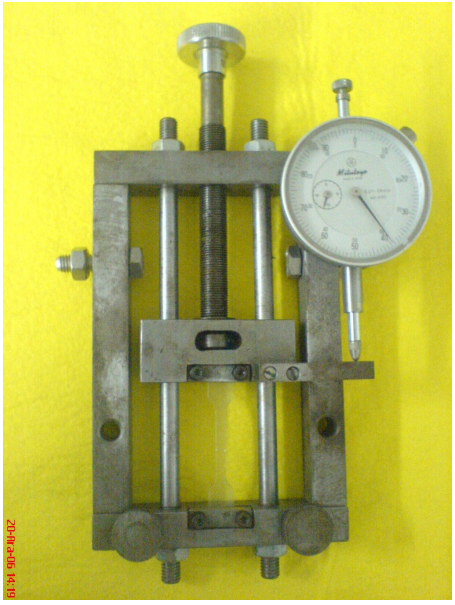

Figure 4.4. Micro-straining device

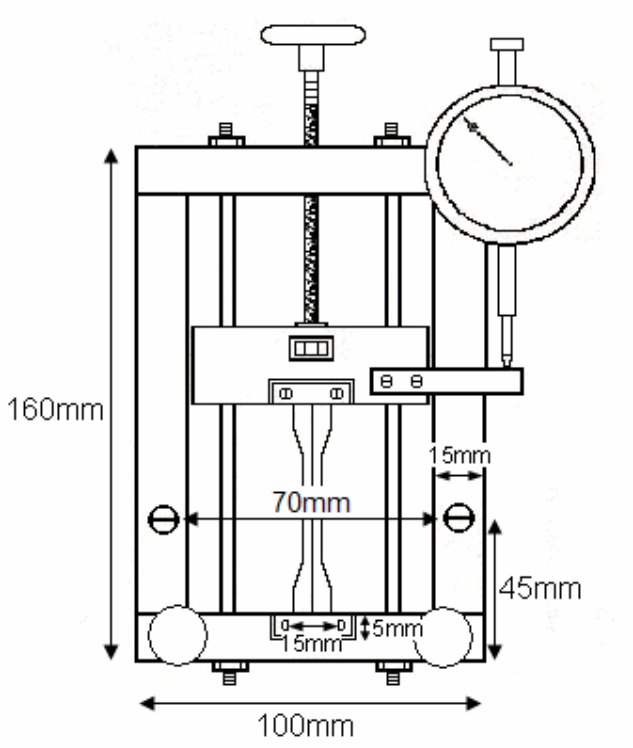

Figure 4.5. Dimensions of micro-straining device

- Baistolscope Bristoline Microscope (200X long working distance objective)
- Digital camera

4.1.3. Characterization Instruments

- H^1 NMR spectra were recorded on a Varian 400 MHz NMR instrument operating at a frequency of 399.986 MHz. The spectra were reported as ppm (δ)

- AFM was performed using an Universal Scanning Probe Microscope (USPM) (Ambios Technolgy, Santa Cruz, CA). Phase mode imaging was performed using a silicone nitride cantilever probe with nominal resonance frequency around 170 kHz and a nominal tip radius of 5-10 nm. Samples were prepared for AFM investigation by mounting the glass fibers in epoxy potting compound. The epoxy was left to cure at room temperature for 24 h.

- Macromechanical tensile tests were done by Cam-Elyaf A.Ş. by universal testing machine, Zwick, with ASTM standards.

4.2. Sample Preparation and Testing

4.2.1. Sample Fabrication

4.2.1.1. Fiber Lay-up.

Fiber lay-up process is the most challenging step. A silicone mold with eight dogbone-shaped cavities was used for the preparation of the test samples. Each cavity in the mold has sprue slots in the center of each end to aid in aligning the fiber in the center of the cavity. At the beginning the silicone mold must be clean. Acetone is used to clean polyester from the cavities of the mold.

To place the fibers into the mold, first 12x4 mm aluminum foil is cut. The distances between the slots of the cavities are marked onto the foil. By using a pick, some glue is applied to the foil.

Then one filament of fiberglass is taken from the strand. To take one filament, a strand that is longer than the cavity of the mold is cut by handling the end of the strand with fingers. It is placed into a peace of foil so that the bundle end projects out from the edge of the foil. Then by using fingers, bundle end is lightly stroked that causes filaments to become separated from each other. Then one filament can be easily pulled from the bundle by using fingers or tweezers. The fiber should only be handled at the ends, so as not to alter the properties of the test sample. A black background is used to see thin fibers easily and a magnifying glass is used.

The tip of the fiber is stuck onto the signs on the foil. This process is applied for each of the 8 fibers. After all eight fibers are sticked on to the foil, it is wrapped into two. By this way all fibers can be stationary.

Then glue is applied into the 8 slots of the cavities on the mold by using pick tip. Fibers are placed into the slots one by one by leaving foiled part out of the mold. Once the glue droplets have hardened, the slots on the opposite side of the cavities are glued and free ends of the fibers are placed into these slots. While waiting the glue to dry, rubber eraser is put on the two sides of the fibers in order to give some tension to the fiber.

4.2.1.2. Matrix Casting and Curing.

12 ml CE-92 mixture was poured into a clean 100 ml beaker. First 0.0382 g of Co-naphthenate was added and mixture was stirred very well. Then 0.1738 g of MEKP was added and the mixture is stirred well. Catalyst and accelerator are both reactive compounds and these components should always be added to the resin separately, making sure that one is completely dissolved before adding the other.

By using a disposable dropper, mixture was transferred in to the mold, but not directly on the fibers or into the gauge area of the cavity. These can cause the fiber microbond and misalignment. Filling should be started from the sides of the head parts of

the cavities. Then by giving a little incline to the mold from one end where resin was being added, the resin slowly diffused through the gage areas to the entire the cavities. For polyester the total volume curing shrinkage is given as 8 per cent (linear 2.33 per cent) [33]. Because of this reason cavities should be overfilled so a meniscus above the resin was observed.

Then mold was cured in air at room temperature for one day. The test coupons can be easily removed from flexible silicone mold by bending the mold from the sides.

4.2.2. Testing and Data Collection

At this stage dumbell shaped test coupons were ready for testing to examine the interfacial adhesive strength.

The fiber fragmentation tests were carried out on a small, hand-operated testing machine that described by Drzal and coworkers. The micro-straining device used in this work was designed by Prof. Selim Küsefoğlu.

Prior to testing a sample the dogbone was marked with two ink marks, spaced 25mm apart to count the fragments after loading manually.

From one end the test coupon was inserted into one grip of the test device and then to the other grip. Then test coupon was tightened by using four screws. By rotating the dial, needle was adjusted to zero.

The micro straining device was placed under the microscope. Then strain was applied to the specimen by turning the large knurled knob manually in controlled increments. By the help of the few trials it was found that for glass fibers 2.5 mm elongation was optimum. So by constant rate the specimen was elongated to 2.5 mm without any observation. Then while looking through the microscope the stage was adjusted by raising and lowering until

the fiber comes into view. Because polyester is transparent it was easy to differentiate the fiber and fractures without any polarized light. Then the fragments were counted and again strain was applied by turning the knob by 0.5mm increments in elongation and this process was continued until the number of fiber breaks within gauge length reached a constant. Last 2 data should be same to decide reaching a constant number. After these 4 observations the maximum value was taken as the resulted data of the test.

SFFT test was made for each of the eight specimens. Q-test was made for maximum and minimum of the eight data [35]. Then average value and standard deviation was calculated.

4.2.3. Test samples with multiple glass fiber

The samples were prepared by using two filaments for one cavity of the mold. Eight test samples with the matrix included 12 ml of CE-92, 0.0191 g of Co-naphthenate and 0.0869 g of MEKP. After curing, samples were tested with SFFT as described before.

4.2.4. Test samples with methacryl silane added matrix

Four sets of test samples were prepared, each has four specimens. They placed into the silicone mold as explained before. For the first set 48 ml of matrix was prepared without methacryl silane as explained before. 10 ml of this matrix mixture was used for first four samples. For 3%-MS-WR-5, 1.1 ml methacryl silane was added and second set was prepared with this matrix mixture by using 10 ml of this mixture. For 5%-MS-WR-5, 0.56 ml of methacryl silane was added to the residual matrix mixture. Third set was prepared by using this matrix mixture. For 10%-MS-WR-5, 0.9 ml of methacryl silane was added to the residual mixture. Last set was prepared by using this matrix mixture.

4.2.5. Aminosilylation of unsaturated polyester

To 50 g of CE-92, 0.5 g of hydroquinone and 4 g of A1100 was added. The mixture was stirred at room temperature for one night under very dry conditions.

Four sets of samples were prepared, each has four specimens. WR-5 fibers were used for the first two sets and unsized glass fibers were used for last two sets. They placed into the silicone mold as explained before. Into 12 ml CE-92, first 0.0382 g of Co-naphthenate was added and the mixture was stirred very well. Then 0.1738 g of MEKP was added and the mixture is stirred well. The matrix was applied onto the first set of WR-5 fibers in the mold. Into 12 ml aminosilylated CE-92, first 0.1528 g of Co-naphthenate was added and the mixture was stirred very well. Then 0.6952 g of MEKP was added and the mixture is stirred well. The matrix was applied onto the second set of WR-5 fibers in the mold. These two matrix were applied to unsized glass fibers also. Curing reactions were carried at 40°C for 2 hours.

^{1}H NMR ($CDCl_3$) δ: 0.6 (-C$\underline{H}_2$-Si-); 1.2 (-Si-O-CH_2-C$\underline{H}_3$); 1.28 (-O-CHC$\underline{H}_3$-CH_2-O-); 1.29 (-NH-CH_2-C$\underline{H}_2$-CH_2-Si-); 3.62 (-NH-CH_2-CH_2-C$\underline{H}_2$-Si-); 3.8 (-O-$CHCH_3$-C$\underline{H}_2$-O-); 4.4 (-O-C$\underline{H}CH_3$-CH_2-O-); 5.21 (-CH=C$\underline{Ha}$Hb); 5.66 (-CH=CHa$\underline{Hb}$); 6.66 (-C$\underline{H}$=CHaHb); 6.83 (-O(C=O)C$\underline{H}$=C$\underline{H}$(C=O)O-); 7.30-7.39 (aromatic protons of styrene); 7.45, 7.66 (aromatic protons of phthalate group).

5. CONCLUSIONS

The single fiber fragmentation test provides a possible easy and cheap way to compare the adhesive strength between the fiber and the matrix within the range of the fragment number near the critical fiber length. The results were compared with the macromechanical test results and they were found to be in the same direction and as the values were very close to each other after lots of trials for different fibers with different sizings. By this way SFFT was found to be precise to be a rapid method for industrial applications.

SFFT was applied to test samples with unsized glass fiber and sized glass fiber that is improper to polyester matrix. Because of the lack of covalent bond that was formed in the interphase between fiber and matrix mainly, these samples showed very low numbers of fragments.

The fiber/matrix adhesion has a strong influence on the failure modes in the fiber fragmentation test. Matrix cracks are induced by fiber breaks for the composite system with strong bonding between fiber and matrix. It was observed that strong interphase causes matrix cracks during SFFT. Also it was observed that any crack on the fiber causes debonding areas around the crack.

Test samples which included two glass fiber filaments showed low number of fragments due to one crack on one of the fibers causes the other carry the all stress alone and it fragmented.

AFM images showed that on the surface of glass fiber, size stayed as droplets, so there are unsized areas between these droplets. By using this information two inventions were done. First one was achieved by adding methacryl silane directly to the matrix mixture with different percentages. It was observed that the interphase quality increased by increasing the amount of methacryl silane. But at a point mechanical properties of matrix reduced and before reaching the critical number of fragments, the matrix was broken. 3-

aminopropyltriethoxysilane addition to unsaturated polyester via Michael addition reaction resulted high interphase quality improvement.

REFERENCES

1. Hull, D., *An Introduction to Composite Materials*, Cambridge University Press, Cambridge, U. K., 1981.

2. Mazumdar, S. K., *Composite Manufacturing: Materials, Products and Process Engineering*, CRC Press LLC, USA, 2002

3. Schwartz, M. M., *Composite Materials*, Prentice Hall PTR, New Jersey, 1996.

4. Loewenstain, K. L., *The Manufacturing Technology of Continuous Glass Fibers*, Elsevier Science Publishing Co., Amsterdam, 1973.

5. Jang, B. Z., *Advanced Polymer Composites*, ASM International, Materials Park, OH, 1994.

6. Şen, S., *Unsaturated Polyester Composites Based on Inorganic Microsphere/ Platelet Binary Filler Systems*, M.S. Thesis, Bogazici University, 1999.

7. *Encyclopedia of Polymer Science and Technology,* Vol. 12, John Wiley & Sons., Canada, 1988.

8. Bascom, W. D., L. T., Drzal, The Surface Properties of Carbon Fibers and Their Adhesion to Organic Polymers, *NASA Contractor Report 4084*, N87-25434, 1987.

9. Tripathi, D., F. R., Jones, Single Fiber Fragmentation Test for Assessing Adhesion in Fibre Reinforced Composites, *Journal of Material Science*, Vol. 33, pp. 1-16, 1998.

10. Rochow, E. G., An Introduction to the Chemistry of the Silicones, John Wiley and Sons, Inc., New York, 1951

11. Gerald, L. W., A Silane Primer: Chemistry and Applications of Alkoxy Silanes, *J. Coat. Tech.*, Vol. 65, pp. 57-60, 1993

12. Kinloch, A. J., Adhesion and Adhesives: Science and Technology, Chapman and Hall, London; New York,1987

13. Tanaka, T., United States Patent, 20060165968, 2003.

14. Kerans, R. J., R. S., Hay, N. J., Pagano, T. A., Parthasarathy, The Role of the Fiber–Matrix Interface in Ceramic Composites. *Am. Ceram. Soc. Bull.*, Vol. 68, No. 2, pp. 429–442, 1989.

15. Narkis, M., J. H., Chen, R. B., Pipes, Review of Methods for Characterization of Interfacial Fiber- Matrix Interactions, *Polymer Composites*, Vol. 9, No. 4, pp. 245 - 251, 1988.

16. Holmes G. A., D. L., Hunston, W. G. McDonough, R. C., Peterson, *Single Fiber Composites: A New Methodology for Determining Interfacial Shear Strength*, ANTEC 2000 Conference Proceedings (Reproduction), Session: T31 – Advanced Composites I, 2000.

17. Holmes, G. A., D. L., Hunston, W. G., McDonough, R. C., Peterson, *A New Methodology For Determining Interfacial Shear Strength In Single Fiber Composites*, Midwest Advanced Materials and Processing Conferences, 2000.

18. Miller, B., P., Muri, L., Rebenfeld, A Microbond Method for Determination of the Shear Strength of a Fiber/Resin Interface, *Compos, Sci. Technol.*, Vol. 28, pp. 17-32, 1987.

19. Marshall, D. B., An Indentation Method for Measuring Matrix-Fiber Frictional Stresses in Ceramic Components, *Comm. Am. Ceram. Soc.*, Vol. 67, No. 12, pp. 259-260, 1984.

20. Marshall, D. B., W. C., Oliver, Measurements of Interfacial Mechanical Properties in Fiber-Reinforced Ceramic Composites, *J. Am. Ceram. Soc*., Vol. 70, No. 8, pp. 542-548, 1987.

21. Kelly, A., W. R., Tyson, Tensile Properties of Fibre-Reinforced Metals: Copper/Tungsten and Copper/Molybdenum, *J. Mech. Phys. Solids,* Vol. 13, pp. 329, 1965.

22. Schultz, J., M., Nardin, Some Physico-Chemical Aspects of the Fibre-Matrix Interphase in Composite Materials, *J. Adhesion*, Vol. 45, pp. 59, 1994.

23. Nardin, M., J., Schultz, Relationship Between Fibre-Matrix Adhesion and the Interfacial Shear Strength in Polymer-Based Composites, *Composite Interfaces,* Vol. 1, No. 2, pp.117, 1993.

24. Rich, M. J., L. T., Drzal, *An Experimental Guide to the Single Filament Coupon Interfacial Shear Strength Test Method*, Lecture notes.

25. Kim, J. K., Y. W., Mai, *Engineered Interfaces in Fiber Reinforced Composites*, Elsevier Science Ltd., Oxford, 1998.

26. Moon, C. K., W. G., McDonough, Multiple Fiber Technique for the Single Fiber Fragmentation Test, *Journal of Applied Polymer Science*, Vol 67, pp. 1701-1709, 1998.

27. Mullin, J. V., J. M., Berry, A., Gatti, Some Fundamental Fracture Mechanisms Applicable to Advanced Filament Reinforced Composites, *Journal of Composite Materials*, Vol. 2, No. 2, pp. 82–90, 1968.

28. Zhoua, X. F., J. A., Nairnb, H. D., Wagnera, Fiber–Matrix Adhesion from the Single-Fiber Composite Test: Nucleation of Interfacial Debonding, *Composites: Part A*, Vol. 30, pp. 1387–1400, 1999.

29. Kim, B. W., J. A., Nairn, Observations of the Fiber Fracture and Interfacial Debonding Phenomena Using the Fragmentation Test in Single Fiber Composites, *Journal of Composite Materials*, Vol. 36, No. 15, pp. 1825, 2002.

30. Mäder, E., S. L., Gao, J. K., Kim, New Nano-scale Characterization Techniques for Interphases, *Proceeding of EUROMAT99-Conference*, Wiley-VCH, New York, 1999.

31. Binning, G., C. G., Quate, C., Gerber, Atomic Force Microscope. *Phys rev lett,* Vol. 56, pp. 930, 1986.

32. Mäder, E., S. L., Gao, Characterization of Interphase Nanoscale Property Variations in Glass Fiber Reinforced Polypropylene and Epoxy Resin Composites, Composites: Part A, Vol. 33, pp. 559, 2002.

33. Dana, D. E., T. C., Huang, E. J., Pepe, United State Patent, 5,091,465, 1992

34. Feih, S., K., Wonsyld, D., Minzari, P., Westermann, H., Lilholt, Establishing a Testing Procedure for the Single Fiber Fragmentation Test, *Risø National Laboratory*, ISBN 87-550-3381-4, 2004

35. Skoog, D. A., D. M., West, *Fundamentals of Analytical Chemistry*, CBS College Publishing, Japan, 1982.